



Cite this: *RSC Adv.*, 2025, **15**, 36249

Received 12th August 2025
 Accepted 16th September 2025

DOI: 10.1039/d5ra05920h
rsc.li/rsc-advances

Recent advances in enyne cycloisomerization using N-heterocyclic carbene gold complexes

Ahmed Hassoon Mageed  *

Since the pioneering discovery of N-heterocyclic carbene (NHC)-gold complexes, extensive research has propelled the field of homogeneous gold catalysis into new frontiers. Among the most dynamic and synthetically valuable applications is the Au(NHC)-catalyzed cycloisomerization of enynes. This review highlights recent advances in this rapidly evolving area, with a focus on the cyclization of 1,6-enynes, 1,5-enynes, and other 1,*n*-enyne systems. Special attention is given to the oxidative cyclization of enynes, which further expands the chemical space accessible *via* gold catalysis. Mechanistic insights are critically examined, revealing how NHC ligands modulate the reactivity, selectivity, and stability of gold centers. Through the lens of both mechanistic understanding and catalytic performance, this review underscores the growing importance of Au(NHC) complexes in the efficient and selective construction of complex molecular frameworks.

Introduction

In 1968, Öfele and Wanzlick introduced the pioneering research on the first N-heterocyclic carbene (NHC) complexes.^{1,2} Subsequently, many NHC-metal complexes have been reported.^{3–11} NHCs display remarkable attributes, such as a robust σ -donor capacity and the capability to establish enduring bonds with main-group and transition metals. In contrast to phosphines, NHCs exhibit improved thermal stability.^{3,12–14} These beneficial properties have propelled the extensive adoption of NHCs as ligands for coordinating various hard and soft transition metals in modern scientific investigations.^{3,8,15–19}

The University of Kufa, Faculty of Science, Department of Chemistry, P. O. Box 21, An-Najaf 54001, Iraq. E-mail: ahmedh.alameri@uokufa.edu.iq



Ahmed Hassoon Mageed

stry, and medicinal chemistry.

N-Heterocyclic carbenes have emerged as versatile ligands for coordinating transition metals, finding diverse applications in catalysis, materials science, and medicinal chemistry.^{9,20–29} Among these transition metals, gold has attracted considerable interest as a distinctive host for NHC coordination due to its unique reactivity and intriguing characteristics.^{30–35} NHC-gold complexes have demonstrated notable catalytic efficacy in a range of synthetic processes, encompassing carbon–carbon bond formation, cross-coupling reactions, and small-molecule activations.^{9,36–41}

In the early 2000s, the first synthesis of NHC-gold complexes marked a significant advancement in the field of gold chemistry.^{42–45} These complexes commonly consist of a chelating NHC ligand bound to a central gold atom, resulting in stable and precisely defined configurations.^{30,32,35,45–48} The potent σ -donating properties of NHC ligands, in conjunction with the soft Lewis acidity of gold, lead to distinctive reactivity patterns and bonding interactions.^{22,30,36,49,50} These features have positioned them as valuable materials in homogeneous catalysis, enabling the creation of efficient and selective transformations.^{37,39,40,50–52} Furthermore, NHC-gold complexes have enabled various organic transformations, such as enyne cycloisomerizations, propargylic ester rearrangements, hydroaminations, and hydrations.^{53–65}

The significant advancements in enyne cycloisomerization using various metal catalysts are highlighted in Fig. 1. It began in 1984 with the first reported metal-catalyzed enyne cycloisomerization by Trost's research group using Pd(II).⁶⁶ In 1988, Grigg's research group introduced Rh(I)-catalyzed enyne cycloisomerization.⁶⁷ The field advanced further in 2000, with Trost's report on Ru(II)-catalyzed enyne cycloisomerization,⁶⁸ followed by Echavarren's discovery of Pt(II)-catalysis in 2001.⁶⁹ In 2004, Echavarren also pioneered the use of Au(I) catalysts for enyne



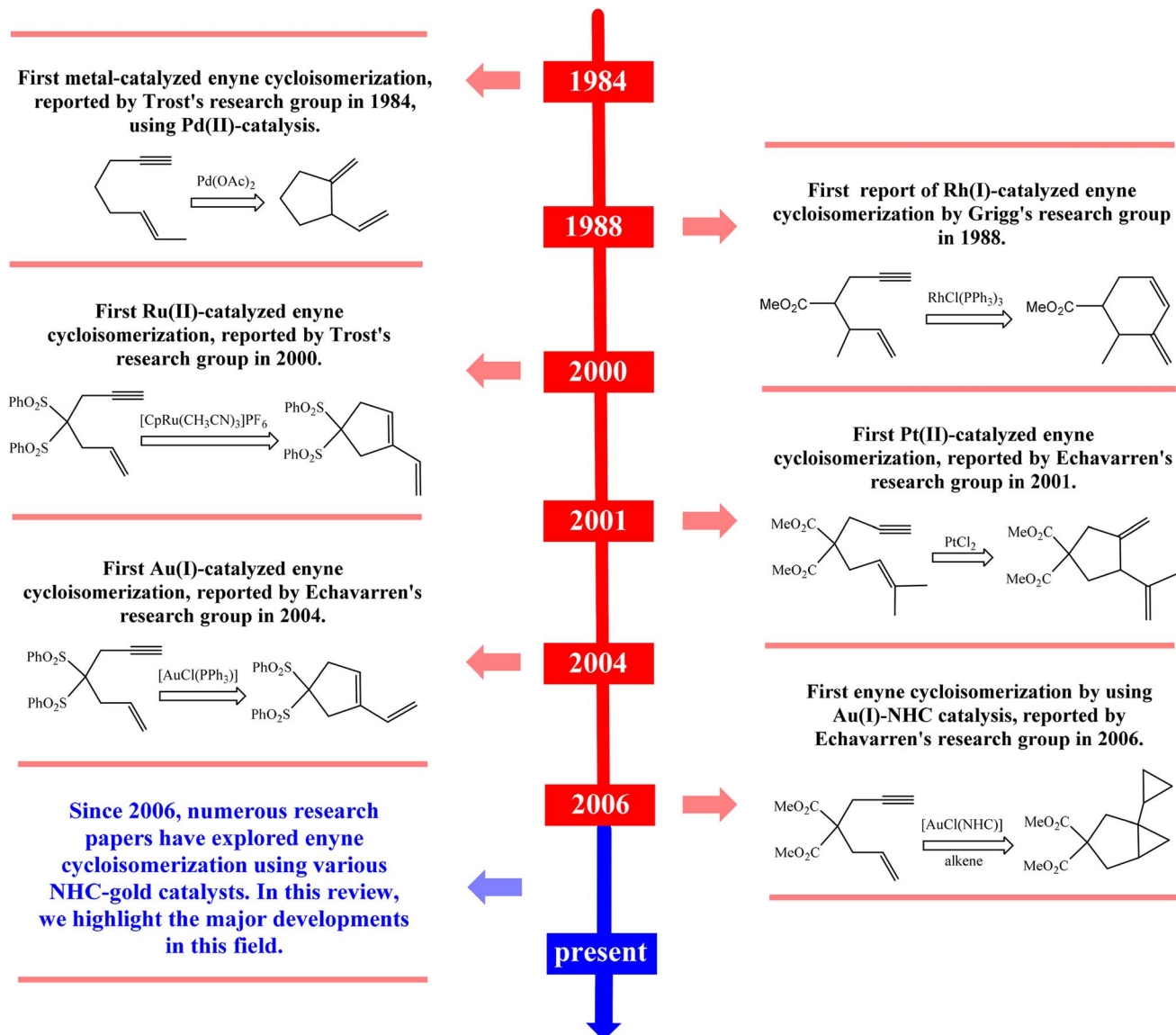


Fig. 1 Key advancements in enyne cycloisomerization using diverse metal catalysts.

cycloisomerization, marking a significant breakthrough.⁷⁰ The next major advancement occurred in 2006 when Echavarren's group introduced Au(I)-NHC catalysts for enyne cycloisomerization.⁵³

Since that seminal work, a wealth of research has explored a variety of NHC-gold complexes, resulting in significant progress in this domain. This review highlights the latest breakthroughs in the Au(NHC)-catalyzed cycloisomerization of 1,*n*-enyne, emphasizing insightful mechanistic pathways and enhanced catalytic efficiency.

Gold-catalyzed enyne cycloisomerization

Cyclization of 1,6-enynes

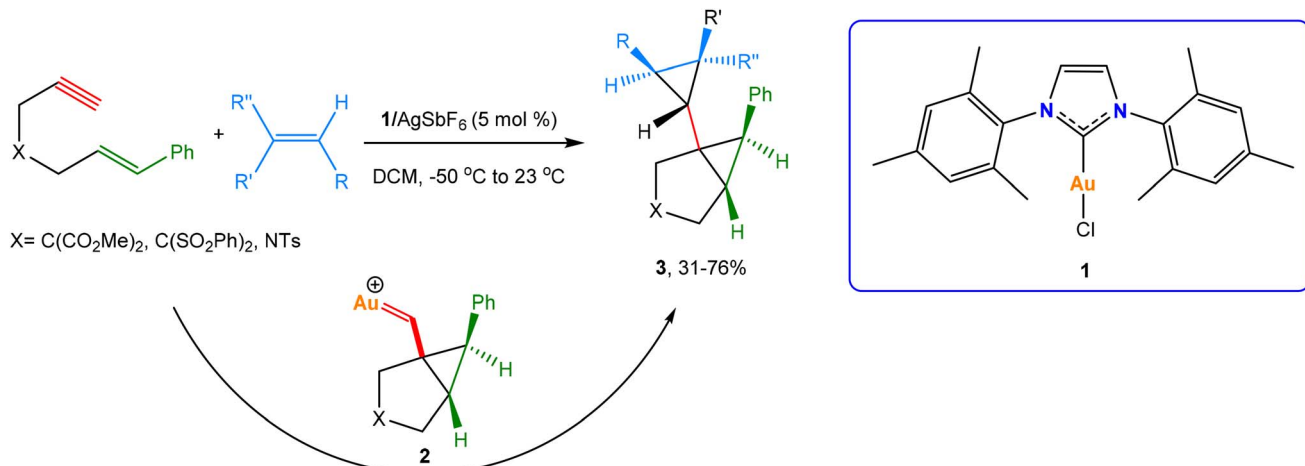
Cyclopropane and polycyclopropane frameworks. In 2006, Echavarren and co-workers reported the first and effective

utilization of IMesAuCl **1** (Scheme 1), along with AgSbF₆, for the intermolecular bis-cyclopropanation of 1,6-enynes with alkenes.⁵³ In this reaction, intramolecular cyclopropanation occurs, leading to the formation of a cyclopropyl gold(I) carbene intermediate **2**. This intermediate is subsequently trapped by an external alkene, resulting in the production of the bis-cyclopropyl compound **3**.⁵³

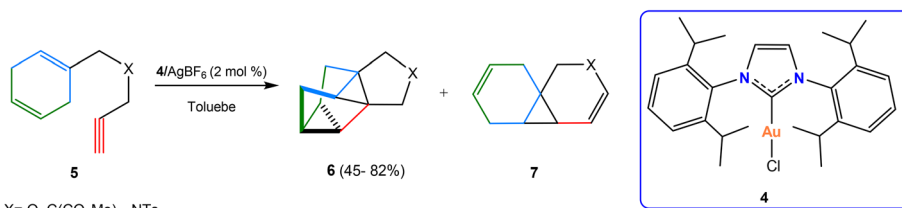
Subsequent studies by Chung and co-workers enabled the synthesis of tetracyclo[3.3.0.0^{2,8}.0^{4,6}]octanes **6** (Scheme 2) using IPrAuCl **4**.⁷¹ These highly strained compounds were derived from the double intramolecular cyclopropanation of 1,6-enynes **5**, which feature a 1,4-cyclohexadiene core, through a cyclopropyl gold(I) carbene intermediate. Optimization studies detected the important role of the solvent and the type of silver salt, particularly in enhancing control over the **6** and **7** selectivity.

Echavarren and co-workers found that the NHC-gold(I) complexes (e.g. **8** or **9** in Scheme 3) catalyzed 1,6-enynes





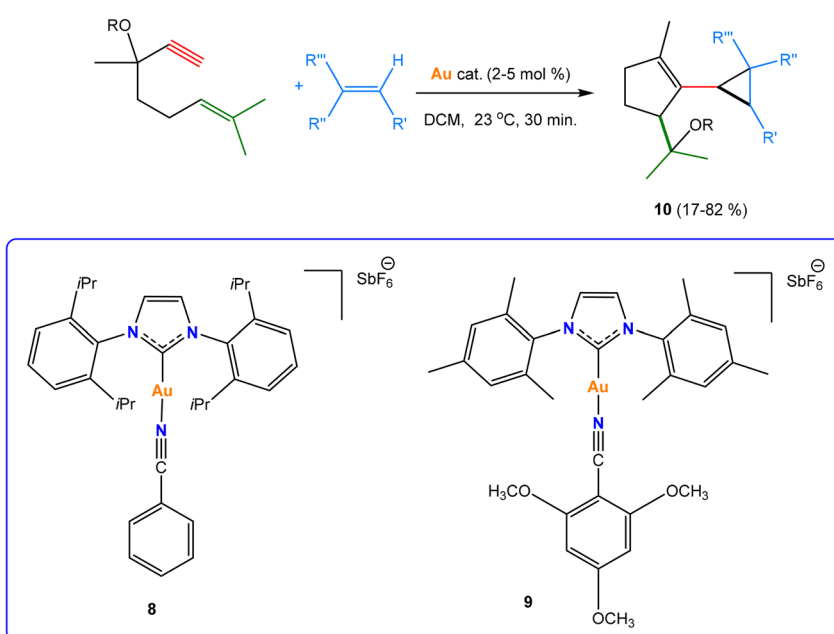
Scheme 1 Cyclopropanation of enynes with alkenes over the NHC–Au(i)–Cl catalyst.



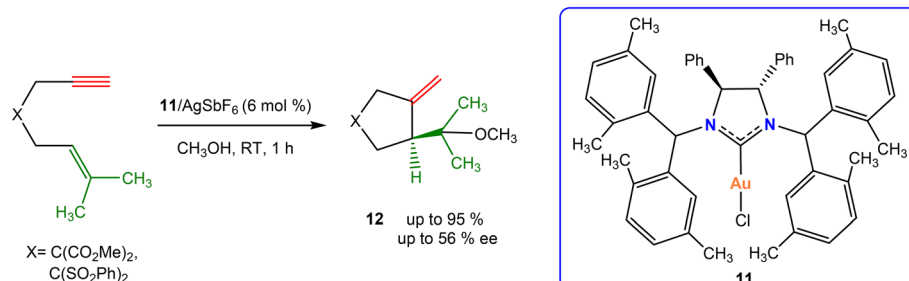
Scheme 2 Intramolecular bis-cyclopropanation, catalysed by NHC–Au(i)–Cl 4.

containing OR groups at the propargyl position to form a cyclopropyl gold(i) carbene intermediate, which can be trapped with alkenes to obtain cyclopropanes **10** after 1,5-OR migration.^{72,73}

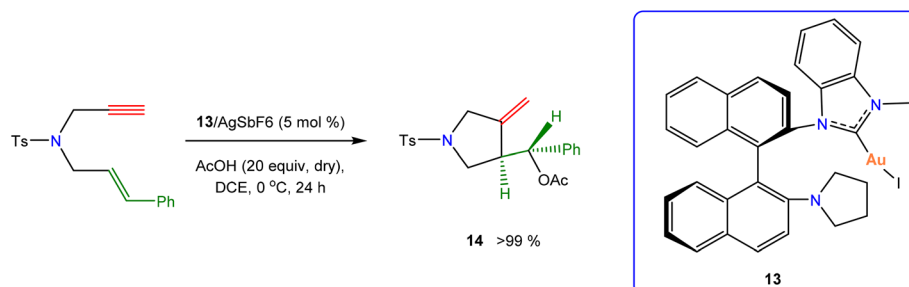
Cyclopentane and cyclopentene derivatives. In 2010, Tomioka and co-workers reported the first example of gold(i) catalysis **11**, including chiral C2-symmetric NHCs, to evaluate their stereocontrolling abilities in the asymmetric cyclization of



Scheme 3 Gold(i)-catalyzed intermolecular cyclopropanation of enynes after 1,5-OR migration.



Scheme 4 The asymmetric cyclization of 1,6-enynes, catalysed by a chiral NHC–gold(i) complex.



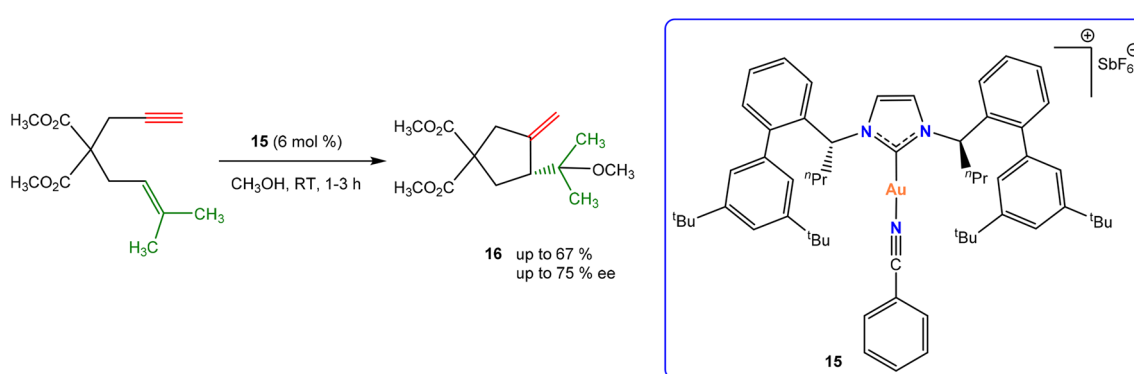
Scheme 5 Intramolecular cyclization of enyne, catalysed by NHC–Au(i)–I 13.

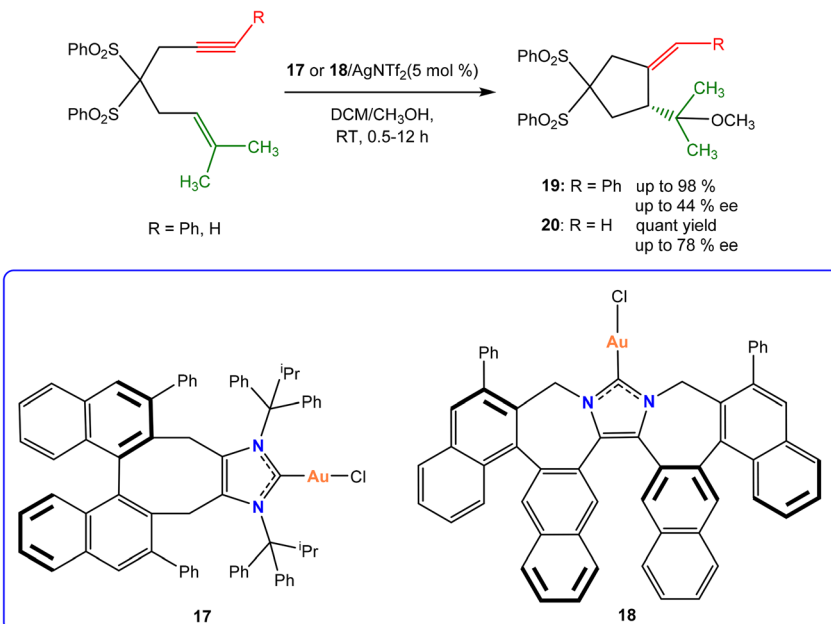
1,6-enynes. This reaction yielded the corresponding cyclopentane derivatives (*e.g.* **12**) in high yields (up to 95%), though with only moderate enantioselectivity (up to 59% ee) (Scheme 4).⁷⁴ Importantly, the study identified structural features—such as the introduction of sterically demanding diarylmethyl substituents—that improved stereocontrol by creating a chiral environment near the metal center.

In 2011, Shi and co-workers reported another NHC–gold(i) complex **13**, featuring a pyrrolidin-1-yl group, which has been identified as the optimal catalyst for the gold(i)-catalyzed asymmetric acetoxycyclization of 1,6-ynye. This catalyst facilitates the formation of product **14** with a yield exceeding 99% and an enantiomeric excess of 59% ee at a temperature of 0 °C (Scheme 5).⁵⁸ A notable strength of this work is the systematic variation of substituents to tune the steric environments around the gold center. The finding that the sterically less

hindered complex **13**, bearing a pyrrolidin-1-yl group, provided excellent chemical yields (>99%) but only moderate enantioselectivity (59% ee) highlights both the promise and the challenge of this catalyst class. It underscores the persistent difficulty of translating the structural chirality of ligands into effective asymmetric induction in gold catalysis, due to the substrate's coordination site being spatially removed from the chiral axis.

In 2016, Gung and his group prepared a number of C2 symmetric NHC ligands, along with their corresponding gold(i) complexes. The newly developed gold complexes were used as catalysts in the cyclization reactions of 1,6-enynes. The NHC–Au(i) complex **15** demonstrated effectiveness in producing the cycloadduct **16** with ee values of up to 75% (Scheme 6).⁷⁵ The study highlighted that the steric bulk of the distal aryl ring in the *ortho*-biphenyl moiety of the ligand is critical for controlling

Scheme 6 Cyclization reactions of 1,6-enynes, catalysed by NHC–Au(i) complex **15**.

Scheme 7 C₂ symmetric NHC gold(I)-catalysed cyclization of 1,6-enynes.

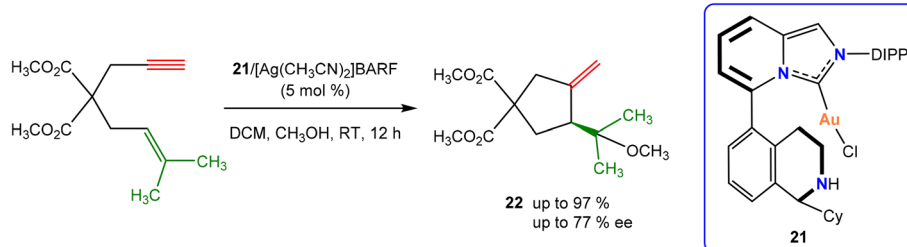
enantioselectivity. Large distal aryl groups generally enhance ee, whereas bulky alkyl substituents can impede substrate access and lower selectivity. Fine-tuning the steric properties of the distal aryl group offers a promising strategy to improve face-selective coordination and overall catalyst performance across different substrates.

In the same year, Nakada and his group synthesized novel C₂ symmetric NHC ligands along with their corresponding gold(I) complexes (**17** and **18**).^{76,77} NHC ligands feature a chiral bisnaphthyl backbone and an *N*-substituted imidazolylidene moiety bonded by an eight-membered ring. These NHC-gold(I) complexes were applied as catalysts for the cyclization of 1,6-ynye, where complex **17** exhibited limited success, yielding cycloadduct **19** with an ee of 44% (Scheme 9). Additionally, using complex **18**, they successfully achieved the asymmetric cyclization of 1,6-ynye, resulting in cycloadduct **20** with an ee of 78% (Scheme 7).

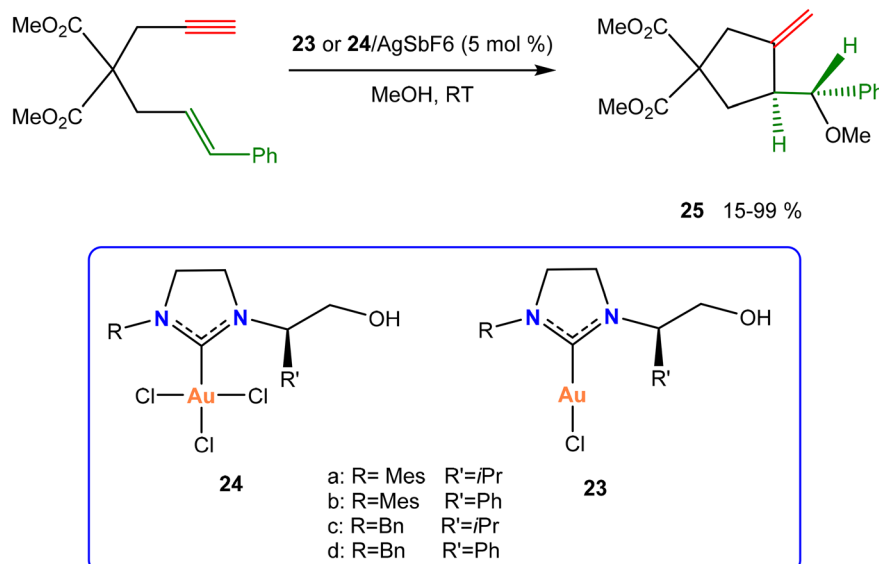
In 2019, Zhang and co-workers reported a chiral bifunctional NHC ligand including an imidazo[1,5-*a*]pyridine (ImPy) moiety.⁷⁸ They explored the applicability of this newly developed ligand in a range of asymmetric gold(I)-catalyzed transformations. Among these transformations, the methoxy

cyclization of 1,6-ynye was successfully carried out using NHC-Au(I) complex **21**, to obtain a cycloadduct **22** with an ee of 77% and a yield of 97% (Scheme 8). Studies on gold-catalyzed alkoxycyclization showed that both the ligand's structure and chirality have a significant impact on the reaction yield and enantioselectivity. Using complex **21** with AgSbF₆ gave a moderate yield (52%) and a low ee (33%). Incorporating the (aS,R)-**21** complex improved both the yield and enantioselectivity (up to ~73%), and the choice of chloride scavenger further influenced selectivity (~77% ee with [Ag(MeCN)₂]⁺ BARF⁻). For sulfonamide-substituted 1,6-enynes, the (aR,R)-**21** complex provided higher yields, although enantioselectivity remained modest, emphasizing the substrate-dependent nature of the ligand performance.

Fiksdahl and co-workers reported a series of chiral gold(I)- and gold(III)-NHC complexes (e.g. **23** and **24**, respectively) derived from chiral amino alcohols. The gold(I)- and gold(III)-NHC complexes were evaluated in an alkoxycyclization test reaction (Scheme 9). The gold(I) complexes **23** exhibited the highest efficiency and selectivity, achieving good yields of the target product **25**. In contrast, the gold(III) complexes **24** provided the fastest conversion but were less selective because



Scheme 8 Chiral bifunctional NHC gold(I)-catalysed cyclization of 1,6-enynes.



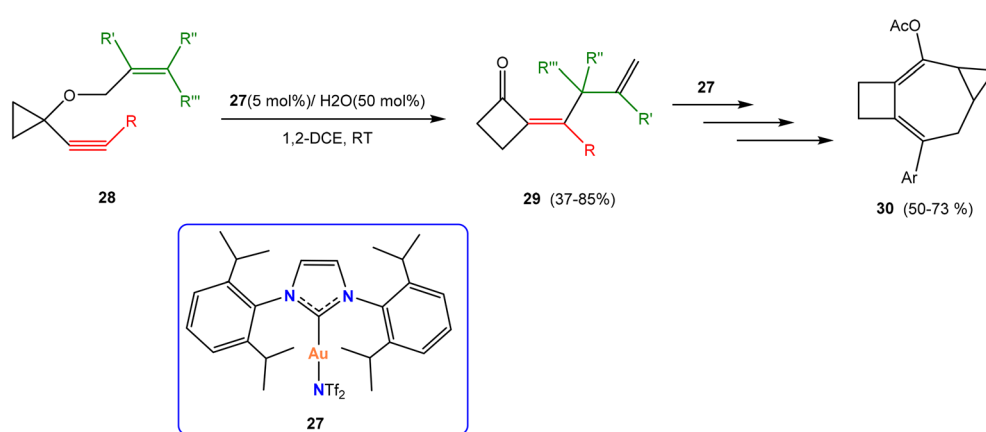
Scheme 9 Alkoxycyclization of 1,6-ene, catalysed by the Au(I)/(III)-NHC complex.

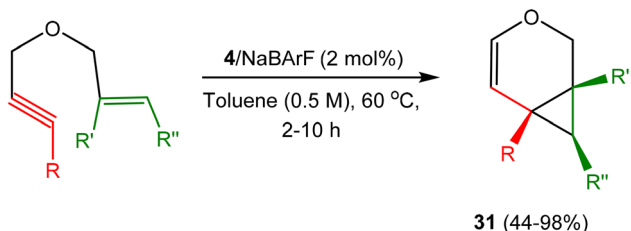
of the competing hydration of the alkyne. Both the gold(I) and gold(III) complexes (23a and 24a), with the bulky N¹-Mes group, demonstrated significantly strong catalytic activity, achieving excellent yields of the target product 25 (92–99%).⁷⁹

Ring-expanded and enol ether products. Fensterbank and co-workers described the cycloisomerization of *O*-tethered 1,6-enynes, catalyzed by NHC-gold(I)-Cl 4, resulting in a small-sized ring expansion and affording 9 examples of enol ethers 26

(Scheme 10).⁸⁰ The introduction of a phenyl group (R = Ph) on the terminal alkyne, combined with catalyst 4, enhanced both yield and selectivity, producing ring-expansion products in moderate to excellent yields. Substrates bearing methyl, isopropyl, or vinyl groups also furnished the expected products, whereas ester-substituted compounds resulted in product mixtures. Acetylenic-cyclopropyl substrates gave very good yields, with stereochemistry confirmed by X-ray analysis. In contrast, substitution at R' with a methyl or prenyl group led to significantly reduced yields of the ring-expansion products.

Shi and co-workers described the NHC-Au(I)-NTf₂ 27-catalyzed ring expansion process that used 1,6-ene alkyneyclopropyl allyl ethers 28 to synthesize tetrasubstituted methylenecyclobutanones 29 in moderate to good yields (Scheme 11). This reaction involved an intramolecular [3,3]-sigmatropic rearrangement, followed by a [1,2]-allyl shift route, facilitated by a catalytic amount of water in the presence of gold(I) catalysis. This interesting mechanism was supported

Scheme 10 Cycloisomerization reaction of *O*-tethered 1,6-enynes, catalyzed by NHC-Au(I)-Cl 4.Scheme 11 Cycloisomerization reaction of 1,6-ene alkyneyclopropyl allyl ethers over NHC-Au(I)-NTf₂ 27.

Scheme 12 Cycloisomerization reaction of *O*-tethered 1,6-enynes.

by various mechanistic experiments and DFT calculations. Additionally, these methylenecyclobutanone products can be transformed into polycyclic skeleton **30** through a practical three-step synthetic procedure under gold catalysis (Scheme 11).⁸¹

In 2020, Michelet *et al.* utilized the cycloisomerization of *O*-tethered 1,6-enynes catalyzed by NHC-gold(i)-Cl **4** to efficiently synthesize 21 examples of volatile enol ethers **31** with unique olfactory characteristics (Scheme 12).⁸² In 2021, the same group reported that **4** demonstrated impressive activities in producing other light bicyclic enol ethers. They successfully synthesized several bicyclic adducts with yields ranging from 18% to 99%. They also evaluated the NHC-Au complexes, achieving a TOF of 300 h⁻¹.⁸³

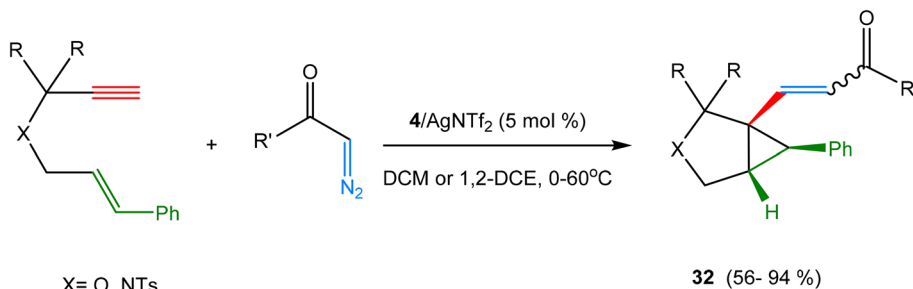
Bicyclic and functionalized frameworks. In 2017, Liu and co-workers reported the synthesis of 21 examples of alkenylicyclopropane derivatives (*e.g.* **32**) from 1,6-enynes and aryl diazo ketones by the cyclization of 1,6-enynes with diazo species (Scheme 13), catalyzed by the NHC-gold(i) complex **4**.⁸⁴ The methodology proved broadly applicable, accommodating a variety of 1,6-enynes and diazo ketones—including *trans*-styryl, cycloalkyl, phenyl, alkyl, and heteroaryl substrates—yielding the desired products in good to excellent yields (56–94%), with most formed as Z/E isomer mixtures.

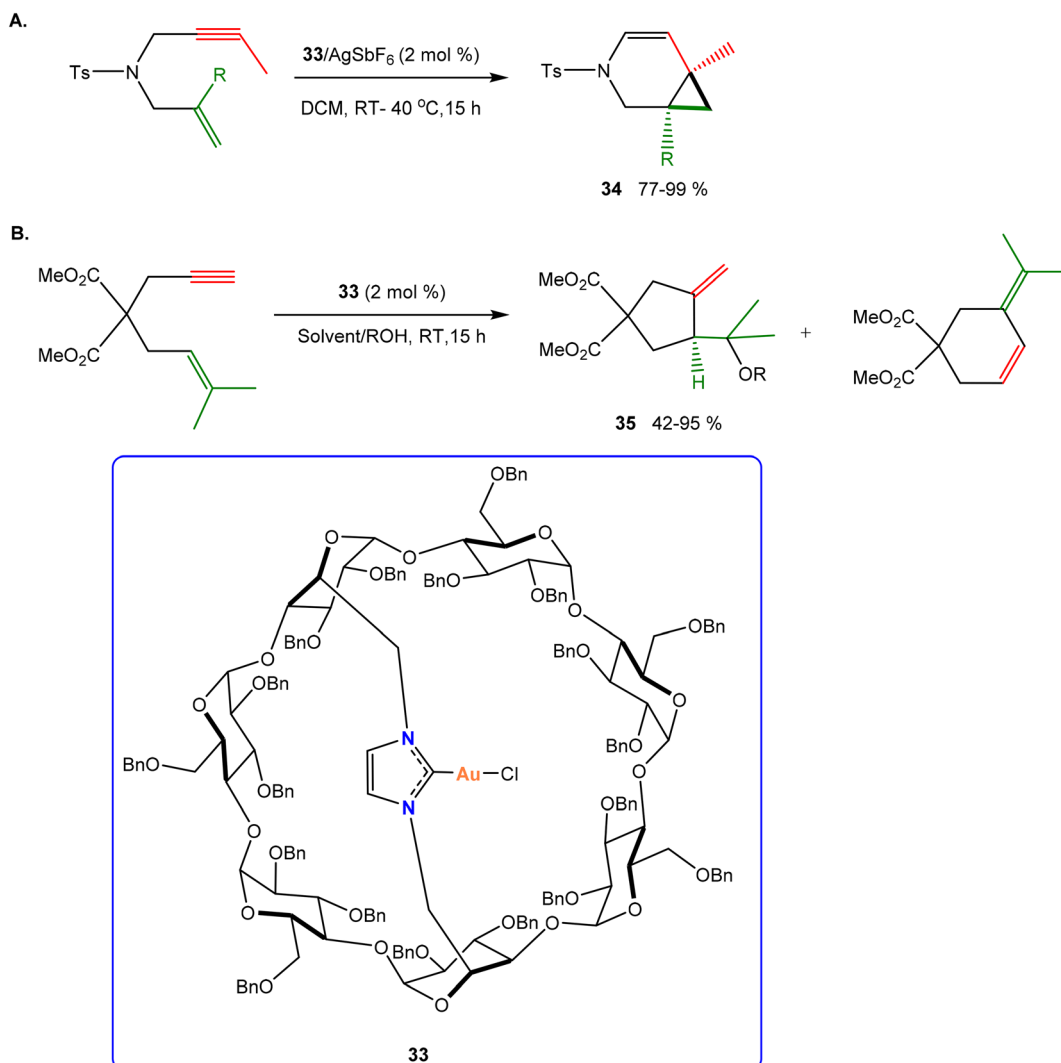
Sollogoub and co-workers were the first to synthesize gold complexes of NHC-capped β -cyclodextrin (β -ICyD) (*e.g.* **33**). The catalytic efficacy of these newly developed gold complexes was showcased through the cycloisomerization of nitrogen-tethered 1,6-enynes to obtain bicyclic products **34** with ee up to 80% and yields up to 99% (Scheme 14A).⁸⁵ In 2020, the same group reported the use of NHC-capped β -cyclodextrin (β -ICyD) as a ligand in gold-catalyzed alkoxycyclization reactions (Scheme 14B). The cyclodextrin component assisted the formation of

a size-exclusive chiral cavity, which permitted only small-sized nucleophiles to enter and engage in gold(i)-catalyzed enantioselective alkoxycyclization, achieving high enantioselectivity of up to 94% ee **35**. It is important to note that larger nucleophiles are unable to access the cavity, and 1,6-ynes would instead undergo intramolecular 6-endo-dig cyclization in the absence of nucleophiles.⁸⁶

Sollogoub and co-workers, in a recent study, introduced a new class of cyclodextrin-based NHC-gold(i) catalysts for the enantioselective cycloisomerization of 1,6-enynes. The study featured three α -cyclodextrin-capped NHC-Au(i) complexes: the perbenzylated (α -ICyD^{Bn})AuCl **36a**; the permethylated (α -ICyD^{Me})AuCl **36b**; and a mixed-substitution variant, (α -ICyD^{Bn,Me})AuCl **36c** (Scheme 15). These ligands were designed to modulate the steric and electronic environment around the metal center by exploiting the structural versatility of cyclodextrin scaffolds. Among the tested complexes, the mixed-substitution complex **36c** displayed superior catalytic performance in terms of both activity and enantioselectivity. The authors attribute this enhanced performance to a well-calibrated balance between steric hindrance and cavity flexibility conferred by the mixed substituents. This structural feature is proposed to create a more favorable chiral environment around the catalytic site, leading to improved asymmetric induction. Indeed, complex **36c** achieved enantioselectivities of up to 86% ee, significantly outperforming both the perbenzylated **36a** and permethylated **36b** analogues, as well as the commonly employed (IPr)AuCl standard catalyst.⁸⁷

In 2022, César and co-workers reported the preparation of the first chiral helicene-NHC gold(i) complexes (*e.g.* **37**) that are effective in enantioselective catalysis. They demonstrated the stereoinducing potential of these enantiopure helical NHC-gold precatalysts in the benchmark Au(i)-catalyzed cycloisomerization of *N*-tethered 1,6-enynes to obtain corresponding bicyclic compounds (*e.g.* **38**) in moderate to good yields (Scheme 16).⁸⁸ Under optimized conditions, a series of *para*-substituted 1,6-enynes underwent smooth cycloisomerization to give bicycles **38** with consistently high enantiomeric ratios (93:7–94.5 : 4.5), independent of the electronic nature of the substituents. Slight yield erosion was observed with electron-withdrawing groups, while bulky substituents such as naphthyl were compatible, providing the desired product in 67% yield with 94:6 er. Overall, this system demonstrated remarkable

Scheme 13 Reactions of diazo ketones and 1,6-enynes over NHC-Au(i)-Cl **4**.



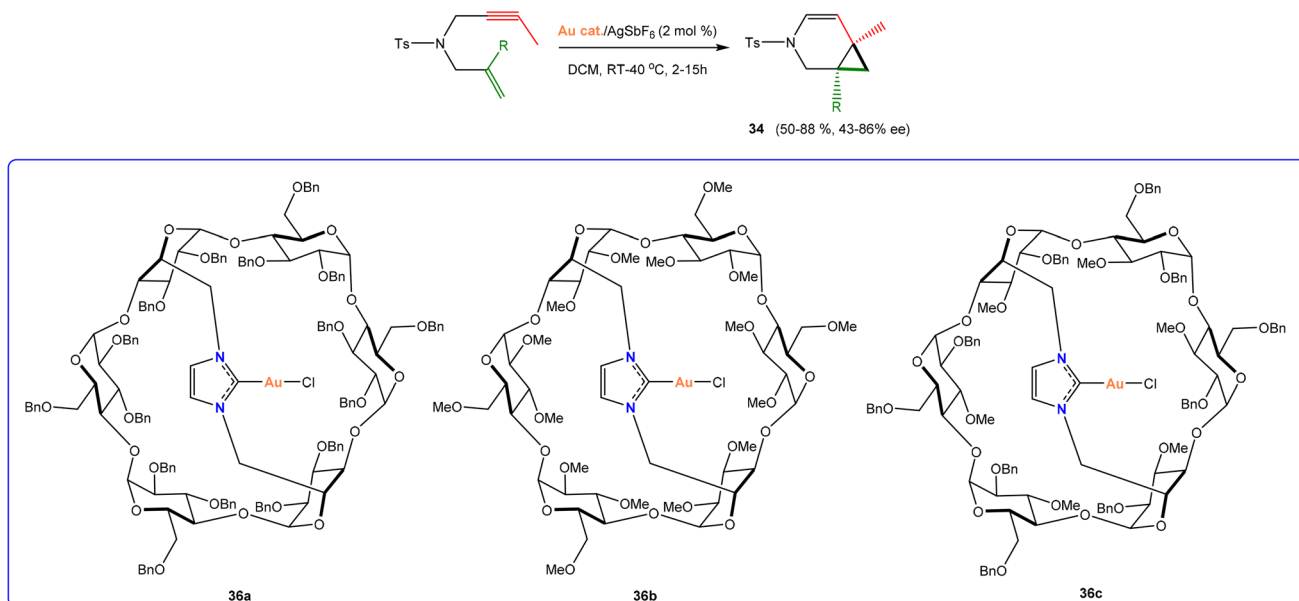
Scheme 14 (A) Cycloisomerization of nitrogen-tethered 1,6-enynes. (B) Enantioselective alkoxycyclization catalysed by $(\beta\text{-ICyD})\text{-NHC-Au(i)-Cl}$.

versatility and efficiency, outperforming earlier Au(i)-based catalytic systems in terms of consistency and substrate scope.

In 2022, Zhao and co-workers reported a NHC-gold(i)-catalyzed cyclization/hydroboration of 1,6-enynes that yielded bicyclo[3.1.0]hexane boranes in moderate to good yields under mild conditions (Scheme 17). This method involves the formation of an *exo*-cyclopropyl gold carbene **40** through the gold-mediated 5-*exo*-dig cyclization of 1,6-enynes. The generated carbene then inserts into the B-H bond of Lewis base-borane adducts *via* transition state **41**, resulting in the desired product **39** and the regeneration of the gold catalyst (Scheme 17).⁸⁹ This strategy provides an efficient, one-step route to boryl-substituted bicyclo[3.1.0]hexanes with a broad substrate scope, high functional group tolerance, and products that are both air-stable and easily purified by chromatography. In addition, the method is amenable to scale-up, and the resulting borane products can be readily diversified, underscoring its strong potential in synthetic chemistry.

In 2023, Zhao and co-workers published findings on a gold-catalyzed Si-H bond insertion reaction involving 1,6-enynes and hydrosilanes (Scheme 18).⁹⁰ This process utilizes cyclopropyl gold carbene intermediates, enabling the straightforward, practical, and atom-economical one-step synthesis of diverse bicyclo[3.1.0]hexane silanes, *e.g.* **42**, achieving moderate to excellent yields of up to 91% under mild conditions. The proposed mechanism begins with the gold catalyst coordinating to the alkyne unit of 1,6-enynes to form intermediate **43**. This intermediate then undergoes a 5-*exo*-dig cyclization, yielding the *exo*-cyclopropyl gold carbene species **44**. Ultimately, this gold carbene inserts into the electron-rich Si-H bond of hydrosilanes, producing the desired bicyclo[3.1.0]hexane silanes **42** and regenerating the gold catalyst (Scheme 18). The method also enables the first example of gold-catalyzed carbene insertion into Ge-H bonds, efficiently affording bicyclo[3.1.0]hexane germanes and further expanding the reaction's synthetic utility.



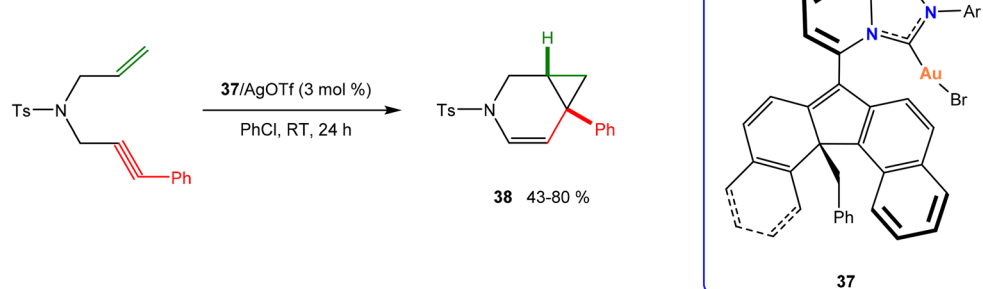
Scheme 15 (α -ICyD)-NHC-gold-catalyzed enantioselective cycloisomerization of enynes.

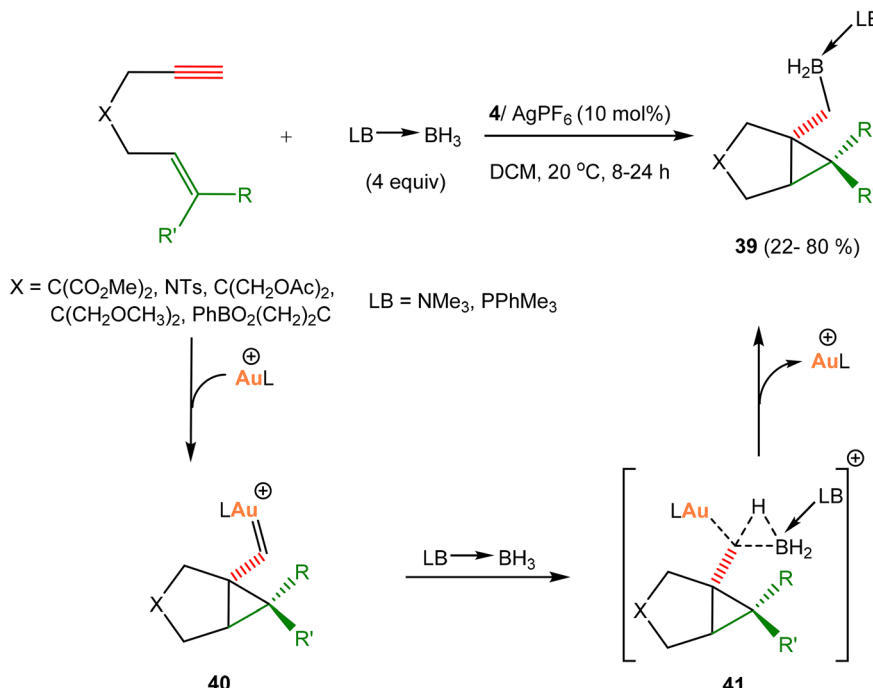
Blanc and co-workers recently demonstrated that NHC–Au(i) complexes (e.g. 46) exhibit catalytic activity in the cycloisomerization of a 1,6-ene 45 in the presence of a silver salt as an activator (Scheme 19).⁹¹ The study revealed that the stereoselectivity of the reaction is significantly influenced by the structural constraints within the ligand framework. The authors showed that the highest enantioselectivity (45a, 72% ee) was obtained when using a benzimidazolin-2-ylidene derivative bearing an (S)-9-(2-hydroxy-1-phenylethyl)fluoren-9-yl *N*-substituent (46). The key factors contributing to this selectivity include the restricted rotation around the N–C_{fluorenyl} bond due to steric hindrance from the bulky NHC plane and the presence of a chiral center at the α -position of the fluorenyl ring. These structural elements play a crucial role in influencing the chiral environment of the catalytic system. The authors suggest that the choice of the silver counterion had a profound impact on the catalytic outcome. Among various silver salts tested, AgOTf provided the best stereoselectivity, likely due to its ability to stabilize the active cationic gold(i) species. The anion (OTf $^-$) is proposed to interact *via* hydrogen bonding with the hydroxyl group on the NHC ligand, thereby rigidifying the catalyst

structure and promoting efficient chirality transfer. This unique mode of activation represents an important development in NHC-gold(i) catalysis, paving the way for further exploration of enantioselective cycloisomerization strategies.

Cyclization of 1,5-enynes. In 2011, Echavarren *et al.* reported that the intermediates in the gold-catalyzed cycloisomerization of 1,5-enynes can exhibit either carbene or carbocationic characteristics. The gold carbenes generated during the cyclization of 1,5-enynes can be trapped by external C-nucleophiles and by pendant alkenes.^{54,55,92,93} The intermediate cyclopropyl gold carbenes (49a or 49b) generated during this cyclization were successfully trapped, resulting in the formation of bicyclic cyclopropane derivatives (47 and 48) through a concerted reaction (Scheme 20).⁹³ They showed, through DFT calculations, that the intramolecular cyclopropanation of 1,5-enynes occurs through a concerted reaction similar to the intra- and intermolecular cyclopropanations observed in reactions involving 1,6-enynes (Scheme 1).

In 2016, Shi and co-workers investigated the NHC–Au(i)-NTf $_2$ complex 27, which effectively catalyzed the cycloisomerization of readily available 1,5-enynes, including a cyclopropane ring,

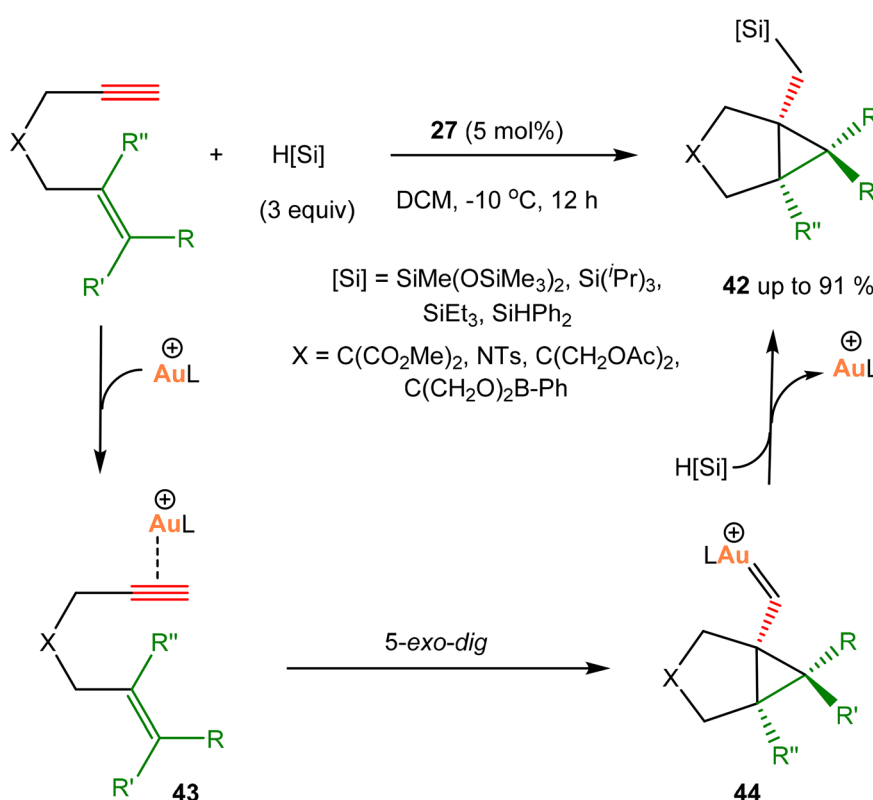
Scheme 16 Cycloisomerization reaction of *N*-tethered 1,6-enynes.



Scheme 17 NHC–gold(i)-catalyzed cyclization/hydroboration of 1,6-enynes.

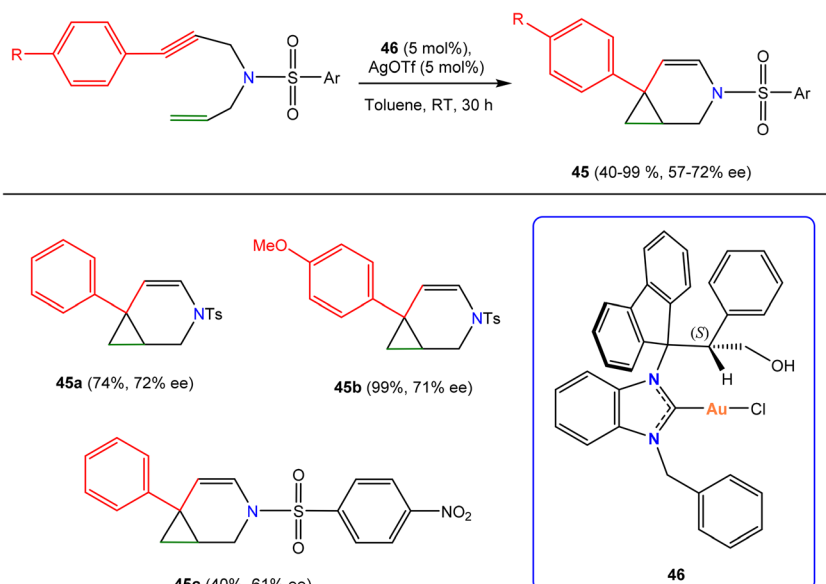
yielding tricyclic cyclobutene derivatives (*e.g.* 50) in moderate to good yields (Scheme 21).⁹⁴ The substrate scope was further evaluated, showing that when the aryl substituent was

a naphthyl, pyrene, or anthracene unit, the corresponding products 50 were obtained in 43–75% yields. Mechanistic investigations, including deuterium-labeling, trapping

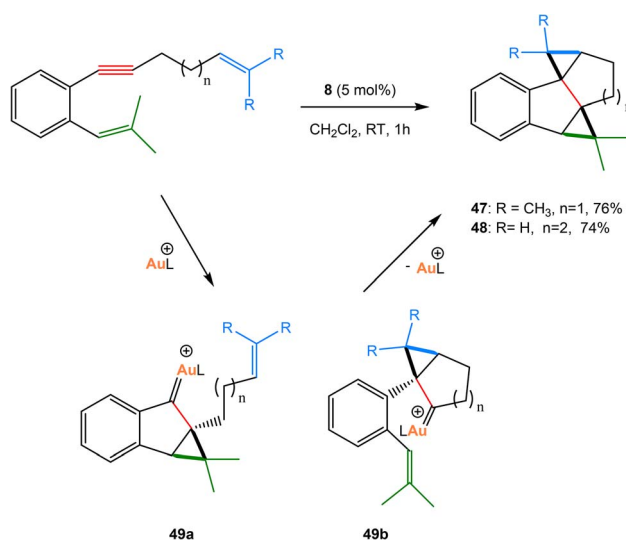


Scheme 18 NHC–gold-catalyzed Si–H bond insertion of carbenes from 1,6-enynes.





Scheme 19 Scope of 1,6-enyne cycloisomerization, catalyzed by the NHC–Au(I) complex 46.



Scheme 20 Cycloisomerization of 1,5-enynes, catalyzed by Au(I)–NHC complexes.

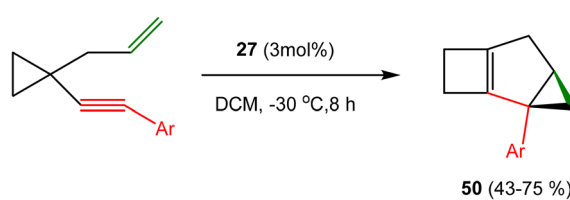
experiments, and DFT calculations, established that the tricyclic cyclobutene functions as the key branching intermediate in divergent reaction pathways. Although the method provides efficient access to structurally diverse frameworks, the substrate scope remains largely aryl-based, and the yields are influenced by steric effects. Importantly, enantioselective variants were not explored, highlighting opportunities for the development of chiral gold catalysts. Overall, this work represents an important mechanistic advance and lays the groundwork for expanding the synthetic utility of Au(I)-catalyzed enyne cycloisomerizations.

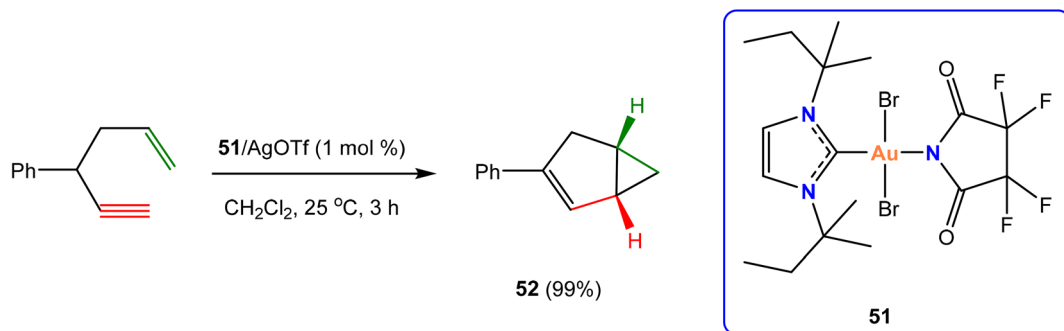
Fairlamb and co-workers investigated the cycloisomerization of 1,5-enynes to test the catalytic activity of the NHC–AuBr₂(N-imide) complexes (e.g. 51, Scheme 22).⁹⁵ The Au(III) imide

complexes demonstrated effective catalytic activity for the cycloisomerization, with the imide ligand playing a key role in enhancing catalytic activity. Complex 51 achieved a high conversion of 52 (99%) (Scheme 22), making it significantly more efficient than the other complexes tested.^{56,57,95}

In 2017, Toste and his colleagues used square-planar chiral NHC-biphenyl-Au(III) catalysts to effectively catalyze an enantioconvergent kinetic resolution of 1,5-enynes. This process afforded bicyclo[3.1.0]-hexenes with enantioselectivities of up to 90% ee, representing the first highly enantioselective transformation achieved using the Au(III)–NHC catalyst (Scheme 23).^{96,97} In a related study, the same group designed an achiral Au(III)–NHC complex 54, which was integrated into a rigid metal–organic framework to geometrically inhibit unwanted decomposition by the reductive elimination of biphenylene.⁹⁸ This complex exhibited catalytic activity, after chloride abstraction by TlPF₆, in the cycloisomerization of 1,5-enyne.⁹⁹

In 2024, Fensterbank and co-workers showed that cavity-driven catalysis with the β -cyclodextrin–NHC–Au(I) complex 33 offers a valuable approach for achieving highly enantioconvergent cycloisomerizations of 1,5-enynes.¹⁰⁰ Interestingly, a remarkable enantioselectivity of 94% was obtained for one of the derivatives of 56 at 0 °C (Scheme 24). The confined catalytic cavity offers a smart design solution, enabling the catalyst to

Scheme 21 Cycloisomerization of 1,5-enynes, catalyzed by the NHC–Au(I)–NTf₂ complex 27.

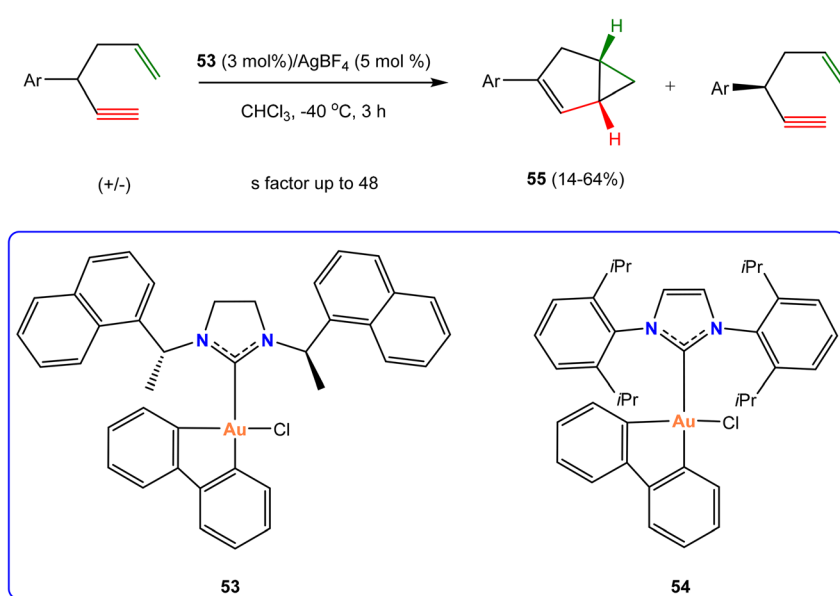
Scheme 22 1,5-Enyne cycloisomerization reaction, catalysed by NHC–AuBr₂(N-imidate) complexes.

overcome substrate-controlled chirality transfer—a long-standing key challenge in gold catalysis. With enantioselectivities reaching up to 94% ee alongside high yields, this approach sets a new benchmark relative to the results achieved with earlier Au(i)- and Pt(II)-based systems. Furthermore, the work underscores the potential of host–guest interactions in supramolecular catalysts as a powerful tool for addressing demanding stereocontrol problems.

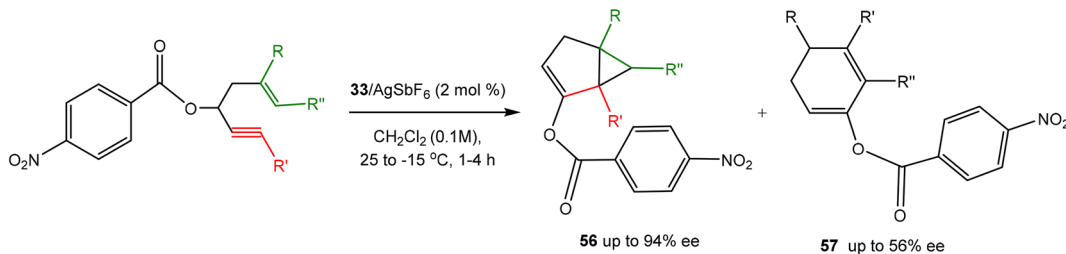
In 2023, Echavarren and co-workers developed two distinct classes of cyclizations utilizing a chiral auxiliary approach with NHC–gold(i) complexes (**58** and **59**) as catalysts (Scheme 25). The first involved the NHC–gold(i)-catalyzed cascade cyclization of 1,5-enynes to obtain spirocyclic compounds (*e.g.* **60**) in high yields. Additionally, they reported NHC–gold(i)-catalyzed alkoxycyclization of 1,6-enynes to obtain the 6-*endo*-dig products (*e.g.* **61**).¹⁰¹

Cyclization of 1,7-enynes. In 2011, Kumar and Waldmann reported a novel 8-*endo*-dig cyclization of 1,7-enynes, catalyzed by an NHC–gold(i) complex **4**. They noted the formation of cyclopropyl-fused compounds **66** in very low yields during the 8-

endo-dig cyclization of 1,7-enynes **62** (Scheme 26).¹⁰² This process involved the coordination of gold(i) to the alkyne, facilitating cyclization and leading to the formation of cationic intermediate **64**. The cationic intermediate was stabilized by the electron-donating effect of the ether oxygen atom, which also promoted the cyclization. Cation **64** either collapsed to form benzoxocine **63** or generated a cyclopropane-substituted gold intermediate **65**, which, upon protodeauration, yielded cyclopropyl-fused compounds **66** (Scheme 26). Overall, this gold(i)-catalyzed 8-*endo*-dig cyclization provides a valuable solution to the long-standing synthetic challenge of constructing benzoxocines, a scaffold central to many biologically active natural products. While the method demonstrates impressive scope and efficiency, key considerations remain regarding stereocontrol, scalability, and compatibility with sensitive functional groups, which will determine its broader applicability. Moving forward, the development of enantioselective variants, integration into cascade or one-pot strategies, and application in total syntheses could make this transformation



Scheme 23 Cycloisomerization of 1,5-enynes, catalyzed by Au(III)–NHC complexes.



Scheme 24 Enantioconvergent cycloisomerizations of 1,5-enynes over β -cyclodextrin–NHC–Au(i) complex 33.

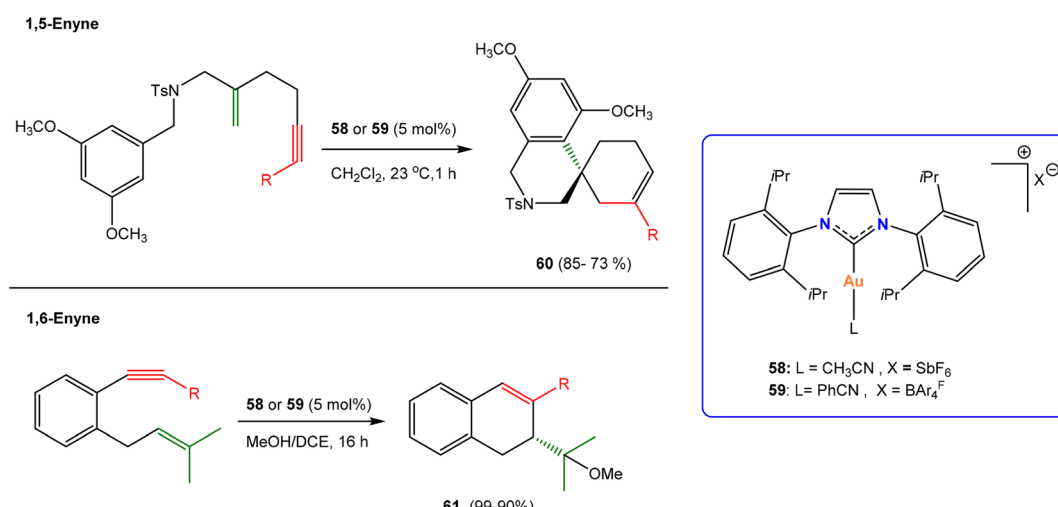
a powerful tool in medicinal chemistry and natural product discovery.

In 2019, Shi and co-workers reported the NHC-gold(i)-catalyzed cascade cyclization of *O*-tethered 1,7-enynes containing a cyclopropane moiety **68**, to obtain highly substituted furans **69** in good yields (Scheme 27).¹⁰³ The proposed mechanism included an intramolecular *O*-nucleophilic attack, followed by a tandem cyclization reaction and a 3,3-sigmatropic rearrangement of the allyl group to produce intermediate **70**. Subsequently, a C–C bond cleavage of the cyclopropane moiety, driven by aromatization in the presence of a cationic gold catalyst, along with further reactions with electrophiles, led to the final products **69** (Scheme 27, route a). Interestingly, for substrates **68** with a methyl or phenyl group at the R'' position, the reaction followed a completely different pathway: the reaction was catalysed by **67** to yield 4-oxaspiro-[bicyclo[4.2.0]octane-2,10-cyclopropan]-1(8)-enes **71** in moderate yields. The substituent on the alkenyl moiety increased its electron density, thereby inhibiting the *O*-nucleophilic attack. As a result, the NHC-gold(i)-catalyzed 1,7-ynye cyclization proceeded to obtain a gold carbenoid intermediate **72**, which then underwent ring expansion to yield the corresponding compound **71** (Scheme 27, route b).

Cyclization of 1,4-enynes. Chan and co-workers explored NHC-gold(i) complex **27**-catalysed 1,4-ynye acetate

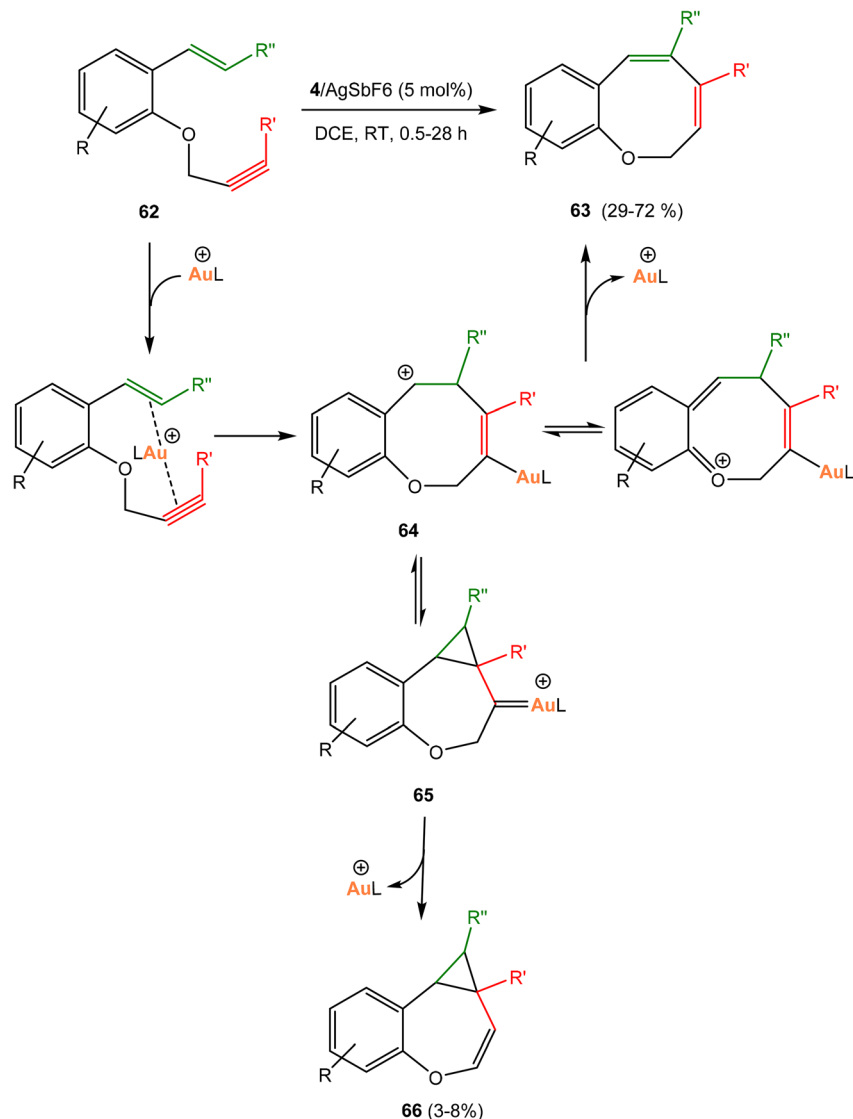
cycloisomerization, followed by oxidation by DDQ, to provide a diverse array of 1*H*-indene products, *e.g.* **74**, containing various substitution patterns. The yields from the corresponding substrates ranged from 22% to 92% (Scheme 28).¹⁰⁴ The proposed mechanism included the activation of the 1,4-ynye motif **73** in the substrate by the gold(i) catalyst, leading to the formation of a gold(i)-coordinated species (Scheme 28). This resulted in a [2,3]-sigmatropic rearrangement of the acetate functional group, producing the cyclopentenium intermediate **75**, which could then afford the 1,3-cyclopentadiene adduct. Further activation of the remaining alkyne group in this adduct by the gold(i) complex could initiate a 6-*endo*-dig cyclization of the resulting organogold species **76**. This process involved the attack of the five-membered carbocycle on the gold-coordinated alkyne motif, affording the bicyclic cation **77**. The subsequent deauration of this cation generated two isomers of dihydro-1*H*-indene under acidic reaction conditions. In the presence of DDQ, the subsequent oxidation of either or a mixture of both isomers produced the aromatic carbocycle **74** (Scheme 28).¹⁰⁴

In 2020, the same group reported the NHC-gold(i) complex **27**- and Brønsted acid-catalysed cycloisomerization of 2- and 3-indolyl tethered 1,4-ynye acetate (*e.g.* **78** and **80**) to obtain spiro [4, *n*]alkyl[*b*]indoles (*n* = 4–6), such as **79** and **81**, under room temperature conditions and in open air (Scheme 29).¹⁰⁵ A broad range of 2-indolyl tethered enyne acetates was examined,



Scheme 25 Cycloisomerization of 1,5-enynes and 1,6-enynes, catalyzed by Au(iii)–NHC complexes.





Scheme 26 Formation of benzoxocines **63** and cyclopropyl-fused compounds **66**, catalyzed by the NHC–Au(*I*) complex.

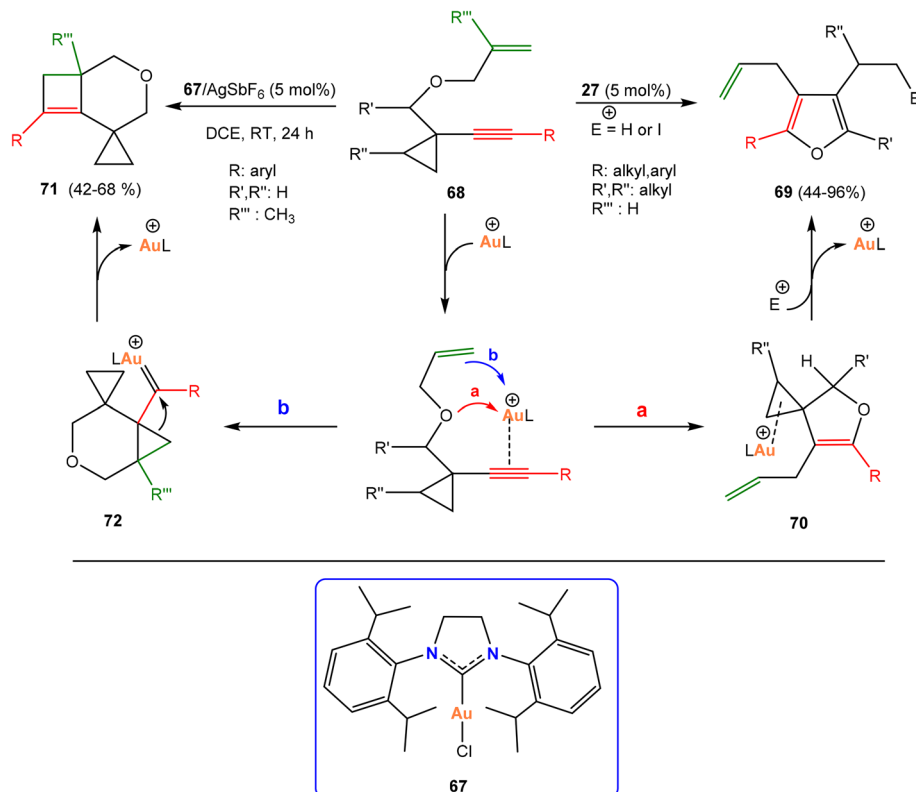
affording indolyl-fused spirocyclic derivatives in moderate to excellent yields (48–91%). The method displayed wide functional group tolerance, accommodating aryl, heteroaryl, and alkyl substituents—including *n*-butyl and cyclohexyl—at the alkynyl position. Substrates bearing electron-donating or electron-withdrawing substituents on the indole ring also underwent smooth cyclization, while variations in N-protecting groups and tether lengths furnished diverse spirocyclic frameworks. Together, these results highlight the robustness, versatility, and generality of this catalytic protocol.

Other enynes. In 2016, Echavarren and co-workers studied the diastereoselective cyclization of (*R*)-**82** to form the 9-membered ring **83** using 5 mol% of catalyst **59**, resulting in a 9 : 1 diastereomeric ratio and a 75% yield (Scheme 30).¹⁰⁶ Among the catalysts examined, complex **59** proved to be the most effective, offering superior yield and selectivity. By contrast, gold(*I*) phosphine complexes provided only moderate yields and lower diastereoselectivity, and they suffered from side reactions,

such as alkyne hydration. The excellent outcome with complex **59** highlights the critical role of the IPr ligand and BAr_4^F counterion in stabilizing the catalytic system and enabling this transformation with much greater efficiency than those provided by the other complexes tested.

Chen and co-workers reported the first example of NHC-gold(*I*) complex **1** catalyzing a formal intermolecular [4 + 2 + 1] cycloaddition using 1,3-dien-8-yne **84** and diazoester **85** (Scheme 31). This approach provides a straightforward method to access a range of structurally complicated [5.3.0] bicyclic adducts, *e.g.* **86**, achieving moderate to high diastereoselectivities. The proposed mechanism highlights the nucleophilic addition of **85** to the cyclopropyl gold carbene intermediate as a crucial step for establishing the quaternary chiral carbon center. This is followed by a Cope rearrangement of the resulting divinyl cyclopropane **87**, leading to the desired [5.3.0] bicyclic compounds **86** (Scheme 31).¹⁰⁷

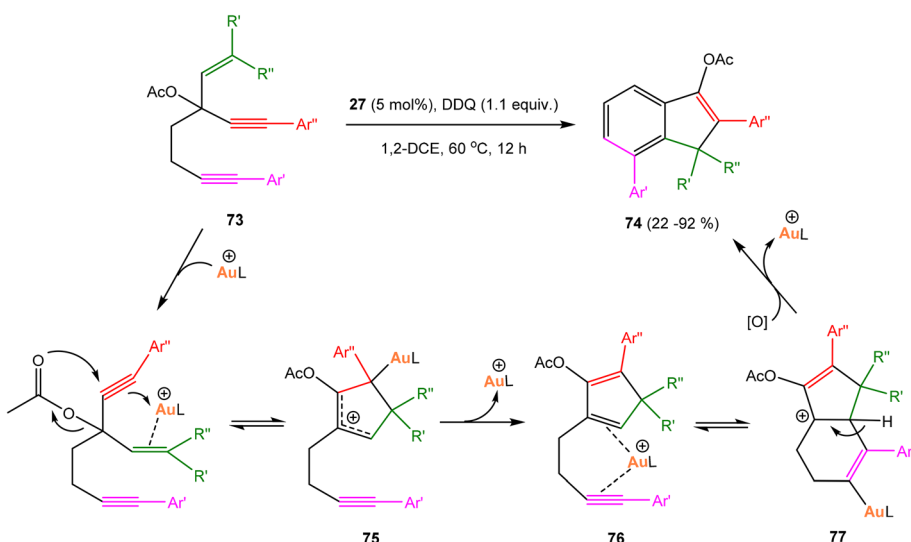


Scheme 27 NHC-gold(I)-catalyzed cascade cyclization of *O*-tethered 1,7-enynes.

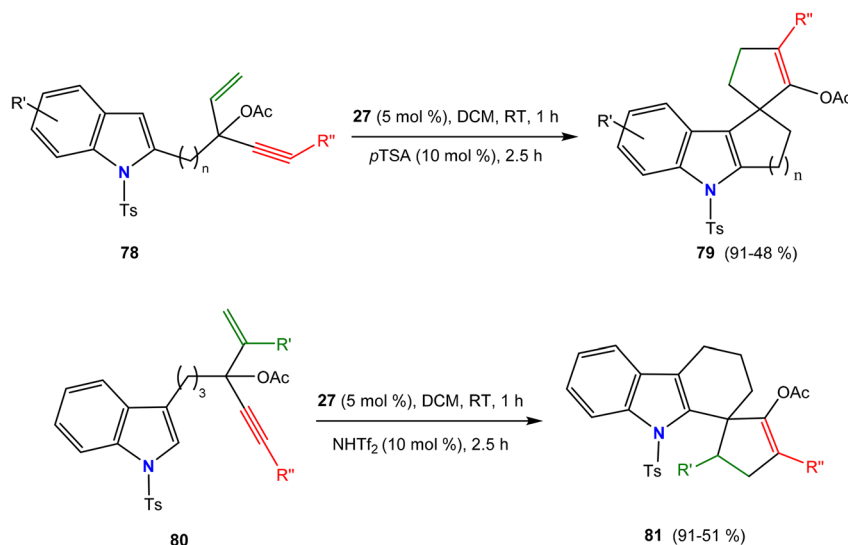
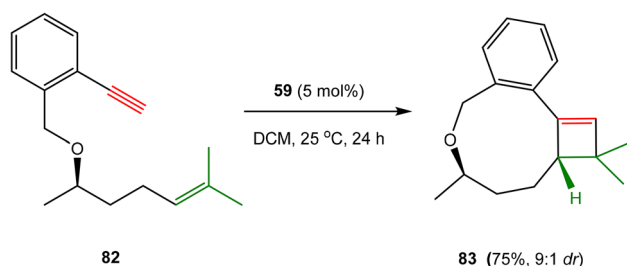
Oxidative cyclization of enynes. In 2007, Toste *et al.* introduced an interesting method for the NHC gold-catalyzed oxidative transformations of alkynes, utilizing sulfoxides as oxidants to produce a range of cyclopropyl aldehydes in high yields.¹⁰⁸ Notably, the carbene nature of the intermediates was confirmed through the transfer of oxygen atoms from a sulfoxide to a cationic gold(I) species. The reaction of 1,6-enynes with two equivalents of diphenylsulfoxide resulted in the

successful synthesis of various cyclopropyl aldehydes **88**, with isolated yields ranging from 90% to 94% and a broad substrate scope. This transformation was achieved using IPrAuCl **4**/ AgSbF_6 (2.5–5 mol%) as the catalyst (Scheme 32).

In the same year, Gagosz *et al.* reported a range of NHC–Au(I)– NTf_2 complexes that have been identified as effective catalysts for various cycloisomerization reactions with enynes.¹⁰⁹ The results achieved with NHC–Au(I)– NTf_2 complexes



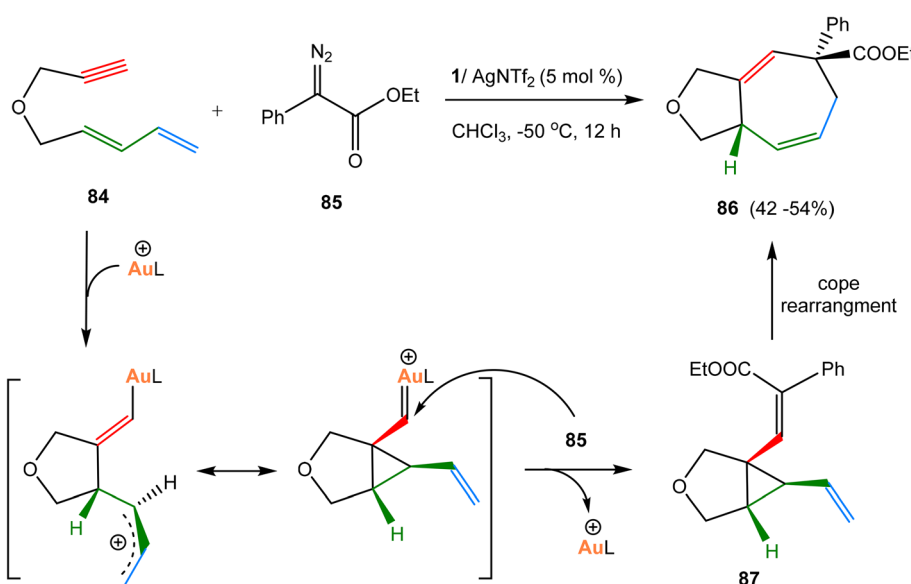
Scheme 28 Cycloisomerization reaction of 1,4-enyne acetates, catalysed by 27.

Scheme 29 Spirocyclization of 1,4-ene, catalysed by **27** and Brønsted acid.

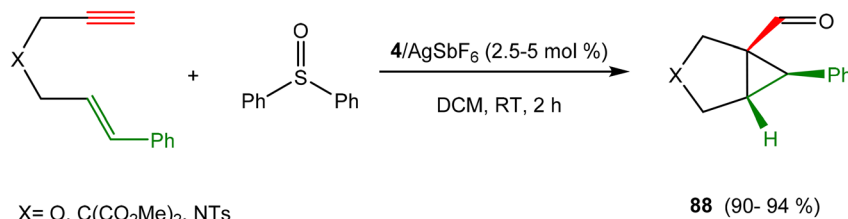
Scheme 30 NHC–gold(i)-catalyzed [2 + 2] cycloaddition of 1,10-enes.

were similar to those obtained with the (NHC–Au(i)–Cl/AgSbF₆) catalytic system reported by the groups of Toste and Echavarren.

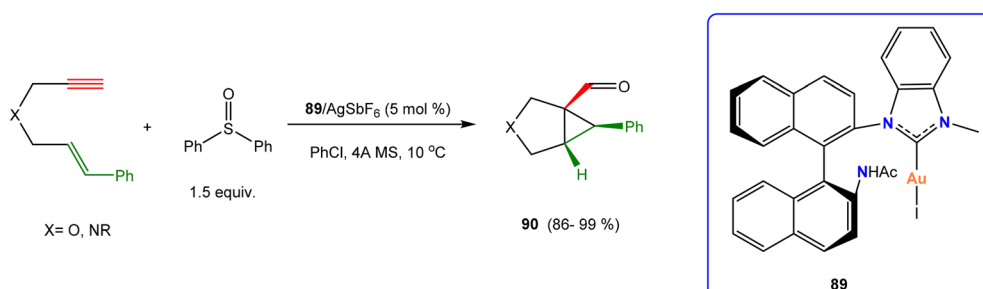
In 2011, Shi and co-workers identified the NHC–gold(i) catalyst **89** as the most effective catalyst for the asymmetric oxidative rearrangement of 1,6-enynes.⁵⁸ This catalyst produced the corresponding aldehydes **90** in high yields, exceeding 99%, and demonstrated moderate enantioselectivities ranging from 3.1% to 70% ee when PhCl was used as the solvent at a temperature of 10 °C (Scheme 33). Further optimization identified Ph₂SO as the optimal oxidant, with the best results achieved under **89**/AgSbF₆ catalysis in anhydrous PhCl at 10 °C in the presence of 4 Å molecular sieves. Under these conditions, aryl-substituted enynes provided products in excellent yields (>99%) with moderate enantioselectivities (58–64% ee). Sulfonyl-substituted enynes displayed more variable outcomes, giving up to 70% ee with 4-bromobenzenesulfonyl but very low enantioselectivities (<11% ee) with bulky or electron-rich



Scheme 31 NHC–gold(i)-catalysed [4 + 2 + 1] cycloaddition of 1,3-dien-8-yne with different diazo esters.



Scheme 32 Synthesis of cyclopropyl aldehydes, catalysed by NHC–Au(I)–Cl 4.

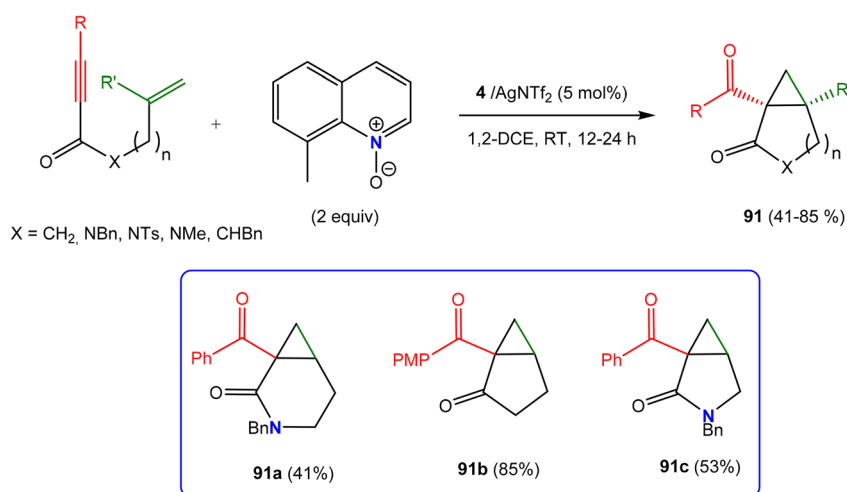


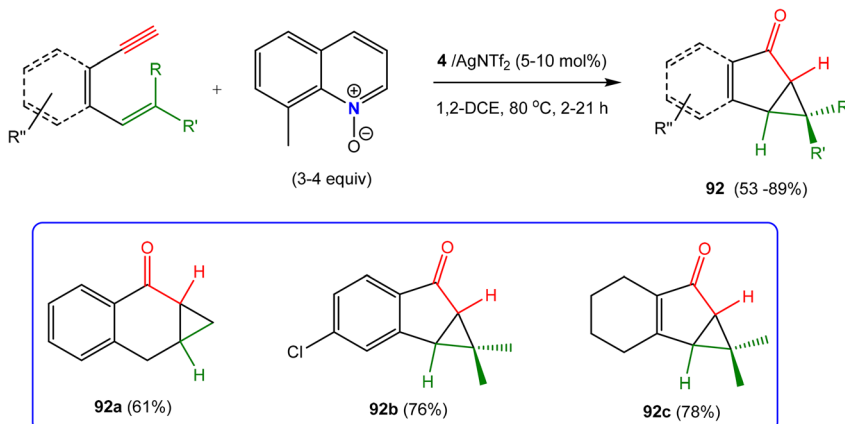
Scheme 33 Synthesis of cyclopropyl aldehydes, catalysed by NHC–Au(I)–I 89.

substituents. Oxygen-tethered enynes also delivered high yields but poor ee, while enynes bearing terminal alkenyl or non-terminal alkynyl groups reacted sluggishly, affording low yields. Overall, these findings demonstrate that while the method is highly efficient in yield, the enantioselectivity is strongly dependent on the steric and electronic nature of the substrate.

In the same year, Qian and Zhang reported a process that involves the cyclization of amide-tethered 1,7-enynes using an NHC–gold(I) catalytic system (**4**/AgNTf₂) and 8-methylquinoline oxide as an oxidant to prepare the [4.1.0] bicyclic compound **91a** (Scheme 34). Additionally, they used the same gold-catalyzed oxidative cyclization of amide- or ketone-tethered 1,6-enynes to produce hetero- and carbo[3.1.0] bicyclic ketones **91**.¹¹⁰ Importantly, 8-methylquinoline *N*-oxide proved to be a particularly effective external oxidant, offering mild, acid-free

conditions; high reaction rates; and room temperature operation. Under these conditions, yields were improved, as demonstrated by product **91c**, whose yield increased from 46% to 53%. The system also showed broad substrate tolerance: both the aryl and alkyl substituents on the alkyne and a range of N-protecting groups (benzyl, sulfonyl, methyl) were well accommodated. Substitution at the alkene moiety was also successful—methylol derivative gave bicyclo[3.1.0]hexan-2-one in a 60% yield with two adjacent quaternary centers, while a benzyl-substituted derivative afforded the product as a mixture of diastereomers. Furthermore, [4.1.0] bicyclic product **91a** was obtained in moderate yield, demonstrating the versatility and synthetic potential of this transformation (Scheme 34).

Scheme 34 Gold(I)-catalyzed oxidative-cyclopropanation of 1,6-enynes and 1,7-enynes using quinoline *N*-oxides.



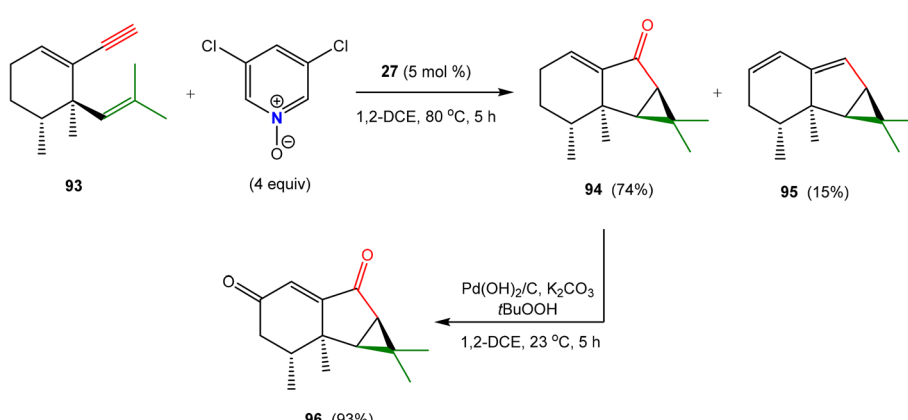
Scheme 35 Gold(I)-catalyzed oxidative cyclization of 1,5-enynes and 1,6-enynes.

In 2011, Liu and co-workers reported the oxidative cyclization of 1,5-enynes, suggesting the formation of α -oxo gold carbenes as intermediates. The 1,5-enynes featuring aromatic or alkenyl linkers yielded cyclopropyl ketones **92** in good yields over a gold **4**-catalyzed reaction, with 8-methylquinoline *N*-oxide as the oxidant. Most reactions required only a 5 mol% catalyst loading and short reaction times, although slightly more stringent conditions were necessary for a substrate with an internal alkyne and for a 1,6-ynye to produce **92a** (Scheme 35).¹¹¹ To evaluate the scope, a wide variety of 1,5-enynes was explored. The methodology proved highly versatile, converting vinyl-, alkyl-, aryl-, and cyclopropyl-substituted enynes into the corresponding indanones in moderate to high yields (53–89%). Trisubstituted alkenes and nonbenzenoid enynes also cyclized efficiently, affording indanone and cyclopentenone derivatives in 61–84% yields (e.g. **92c**). Furthermore, phenyl-substituted enynes with chloro or methoxy groups provided products in 67–76% yields (e.g. **92b**), highlighting the broad substrate scope, functional group tolerance, and generality of this oxidative cyclization.

In 2014, Bielawski *et al.* reported a series of NHCs as ligands in gold(I)-catalyzed 1,6-ynye cycloisomerization reactions to investigate the impacts of ligand steric and electronic effects on

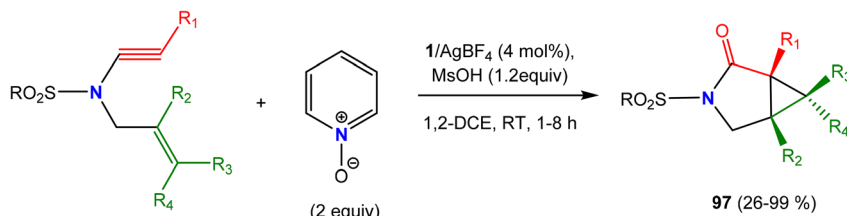
the resulting product mixtures.⁶⁰ The results obtained with the NHC-Au(I)-Cl complexes were similar to those achieved with the (NHC-Au(I)-Cl/AgSbF₆) catalytic system reported by Shi's group. Nevertheless, their results showed that the major product in the NHC-gold(I)-catalyzed 1,6-ynye cycloisomerization reactions was the fused bicyclic products (e.g. **88**).

In 2015, Echavarren and colleagues reported the gold(I)-catalyzed oxidative cyclization of enantioenriched 1,5-enynes **93** using 3,5-dichloropyridine *N*-oxide as the oxidant. This reaction produced the desired product **94** in good yield (74%), along with 15% of the cycloisomerized product **95**. The final step involved allylic oxidation, which enabled the high-yield total synthesis of (–)-nardoaristolone B **96** (93%) (Scheme 36).¹¹² Earlier studies using **27** with 8-methylquinoline *N*-oxide had delivered only modest results, giving 20% of the oxidative cyclization product and 25% of the cycloisomerization product. Careful optimization revealed the crucial role of the oxidant: 3,5-dichloropyridine *N*-oxide proved optimal, while its isomer 2,6-dichloropyridine *N*-oxide exclusively afforded the diene **95** in a 55% yield. The formation of both oxidative and cycloisomerization products suggests a common cyclopropyl gold(I) intermediate, although an alternative pathway involving early



Scheme 36 Gold(I)-catalyzed oxidative cyclization of 1,5-ynye in the synthesis of (–)-nardoaristolone B.



Scheme 37 Gold-catalyzed oxidative cyclopropanation of *N*-allyl ynamides.

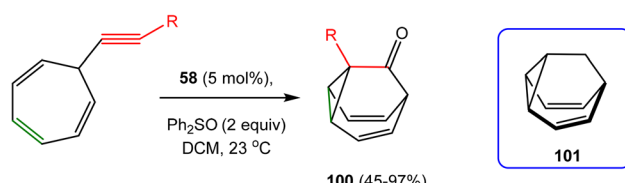
oxidation to an α -oxo gold carbene followed by intramolecular cyclopropanation cannot be excluded.

In 2013, Li and co-workers reported the gold-catalyzed oxidative cyclopropanation of *N*-allylnamide using $1/\text{AgBF}_4$ as the catalyst and pyridine *N*-oxide as the oxidant, yielding various 3-aza-bicyclo[3.1.0]-hexan-2-one derivatives, *e.g.* 97, in moderate to excellent yields (Scheme 37).¹¹³ The reaction showed a broad substrate scope, tolerating various protecting groups (Ms, Ns, 2-trimethylsilylethanesulfonyl (SES), *p*-MeOC₅H₄SO₂, *p*-BrC₆H₄SO₂) and enabling further synthetic flexibility. Both terminal and substituted alkynes proved suitable: the terminal alkyne gave an 85% yield, while the TMS-substituted analogue delivered a 90% yield after desilylation. Halogen substituents (Br, F) and carbonyl-substituted derivatives were also efficiently converted. Substrates with differently substituted allyl units yielded products with vicinal quaternary centers in high yield, though steric hindrance in some cases led to 1,2-dicarbonyl by-products. Electron-rich aryl alkynes similarly favored dicarbonyl formation, highlighting the influence of electronic effects. Notably, reactions with phenyl- or methyl-substituted alkenes yielded exclusively the *trans*-isomer, demonstrating excellent stereoselectivity.

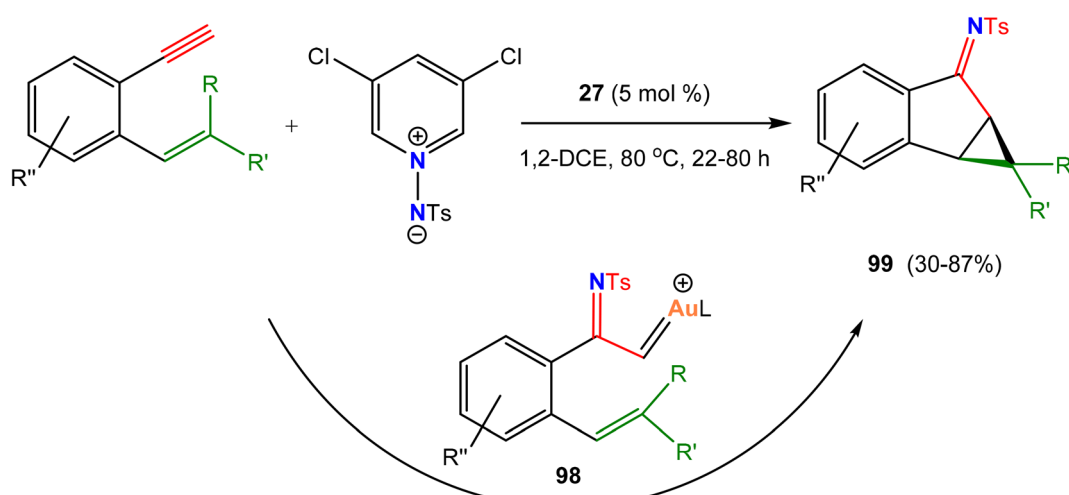
In the same year, Liu and colleagues reported the efficient synthesis of cyclopropyl-indanimines 99 by treating 1,5-enynes with *N*-iminopyridinium ylide (1.2 equiv.) in heated 1,2-dichloroethane (DCE, 80 °C), in the presence of catalyst 27 (5 mol%). The resulting imine products, *e.g.*, 99, were obtained

in yields ranging from 30% to 87% (Scheme 38).¹¹⁴ Notably, a gold carbene intermediate 98 was proposed as the key intermediate, based on prior studies on the oxidative cyclopropanation of 1,5-enynes.¹¹¹ Substrates bearing cyclopentylidene and cyclohexylidene groups gave high yields (85–87%), while stereospecific transformations of regioisomeric enynes supported a gold carbene intermediate. Halogen-substituted enynes (Cl, F) furnished products in 68–77% yields, though electron-rich substrates, such as methoxy derivatives, were less efficient, with one example affording only a 30% yield and another failing due to insufficient alkyne activation.

Echavarren and coworkers demonstrated the efficient synthesis of 17 examples of 1-substituted barbaralone 100 through gold(i) 58-catalyzed oxidative cyclization of 7-(substituted ethynyl)-1,3,5-cycloheptatrienes (Scheme 39).¹¹⁵ This method enables the shortest synthesis of bullvalene and its



Scheme 39 NHC–Au(i)-catalyzed oxidative reaction of 7-ethynyl-1,3,5-cycloheptatrienes to form 1-substituted barbaralone.



Scheme 38 NHC–Au(i)-catalyzed iminocyclization of various 1,5-enynes.

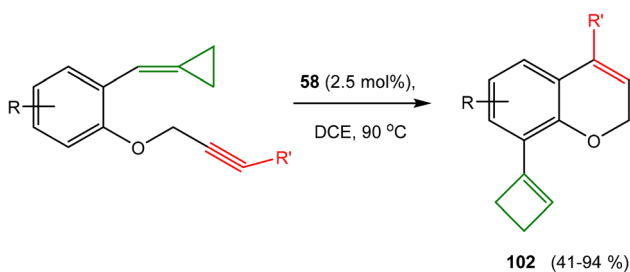


derivatives, with the parent bullvalene **101** obtained in five steps from commercially available starting materials, achieving a 10% overall yield. This represents a significant improvement over previous methods, which required nine or more steps with lower efficiency. The straightforward access to barbaralones facilitates the construction of complex cage systems with novel molecular architectures.^{115,116}

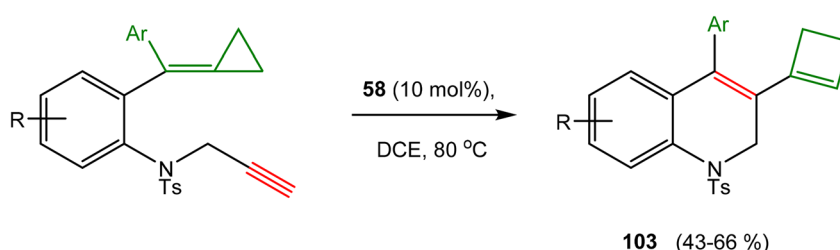
In 2016, Shi and coworkers used a NHC-gold(i)-catalyzed method for converting aryl propargyl ethers into *2H*-chromene derivatives **102** through intramolecular hydroarylation with high efficiency. Additionally, it has been demonstrated that *2H*-

chromene derivatives **102** containing a methylenecyclopropane moiety can undergo further transformation into cyclobutenes *via* ring enlargement under gold(i) catalysis using **58** (Scheme 40). This provides an alternative and effective approach for cyclobutene synthesis.¹¹⁷ The substrate scope demonstrated good generality: aryl propargyl ethers bearing methyl or halogen substituents (F, Cl, Br) on the benzene ring afforded cyclobutenes in moderate yields (41–64%). The substituent effects were clear—*para*-methyl groups increased the electron density at C3, enhancing hydroarylation and giving higher yields than *meta*-methyl analogues, while *para*-chloro groups lowered the electron density and reduced the yields compared to their *meta*-substituted counterparts. A phenyl substituent at the terminal alkyne provided cyclobutene in good yield (76%). In contrast, substrates bearing strongly electron-withdrawing (*m*-NO₂) or electron-donating (*p*-MeO) groups, as well as those with ester substituents (R' = CO₂Et), afforded complex mixtures, likely due to unfavorable electronic effects.

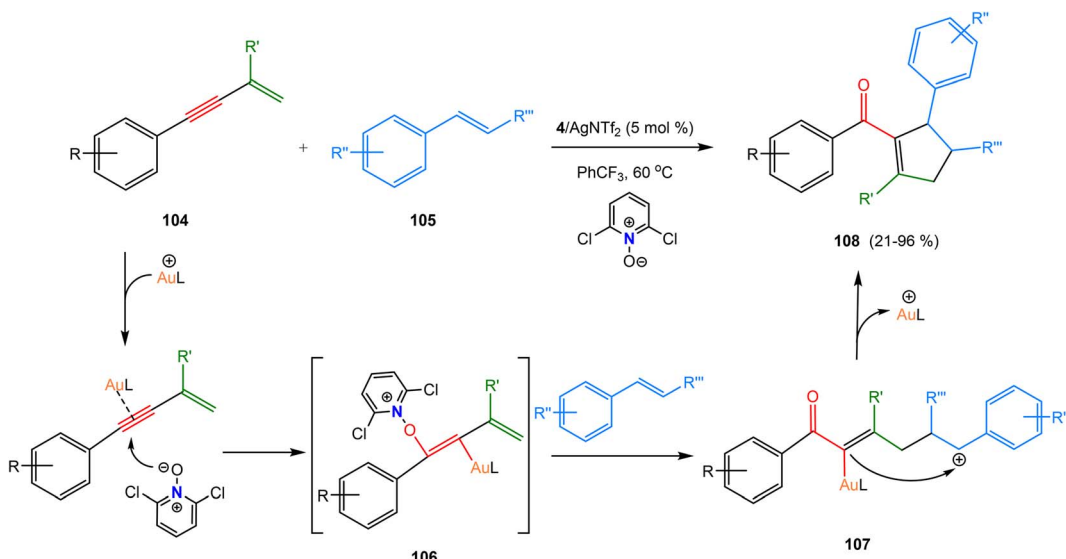
In 2018, the same group reported NHC-gold-catalyzed annulations of aniline-linked 1,7-enynes containing a methylenecyclopropane, yielding 1,2-dihydroquinoline derivatives **103** in moderate yields under mild conditions (Scheme 41). The formation of 1,2-dihydroquinolines bearing a cyclobutene moiety may proceed through a cyclopropyl gold–carbene



Scheme 40 Conversion of aryl propargyl ethers into *2H*-chromene derivatives *via* **58**.



Scheme 41 NHC-gold-catalyzed intramolecular annulation of aniline-linked 1,7-enynes.



Scheme 42 NHC–gold-catalyzed [3 + 2] cycloaddition of 1,3-ynes with different aryl olefins.



intermediate formed twice during the process.¹¹⁸ Substrates bearing electron-withdrawing halogens on both aromatic rings afforded hydroquinoline products in 51–63% total yields, while alkyl- and naphthyl-substituted derivatives provided the product in 41–66% yields. A *meta*-methoxy substituent gave a moderate yield (61%), whereas *ortho*- and *para*-methoxy groups led only to complex mixtures, highlighting the strong positional effect of electron-rich substituents. Similarly, heteroaryl substrates (furan and thiophene) in this reaction gave only complex mixtures, and no reaction was observed under the standard conditions. In all successful cases, the hydroquinoline products **103** were consistently obtained as the major products.

In 2024, Chen and co-workers synthesized cyclopentenyl compounds by employing a NHC-gold-catalyzed reaction of 1,3-enynes with various olefins in the presence of pyridine *N*-oxide as the oxidant. Notably, when reacting 1,3-enynes with aryl olefins, they successfully produced a range of cyclopentenyl ketone derivatives (*e.g.* **108**) through a formal [3 + 2] cycloaddition (Scheme 42).¹¹⁹ The authors proposed a reaction mechanism, which is depicted in (Scheme 42). Initially, the gold-containing *N*-dienoxypyridinium intermediate **106** is formed *in situ* by the addition of an *N*-oxide to the gold-activated 1,3-enyne **104**. This process generates the vinyl-gold carbocation intermediate **107**, formed from the **105** reaction, whose stability is enhanced by the neighboring phenyl group. The stabilized carbocation undergoes intramolecular cyclization through an interaction with the vinyl-gold bond, ultimately producing the formal [3 + 2] cycloadduct **108**.

Conclusions

The field of Au(NHC)-catalyzed cycloisomerization of enynes has witnessed remarkable growth, driven by the unique properties of NHC ligands and the exceptional reactivity of gold complexes. As demonstrated across a variety of systems—including 1,6-enynes, 1,5-enynes, other 1,*n*-enynes, and oxidative cyclization pathways—these transformations offer powerful, atom-economical routes to structurally diverse and complex cyclic frameworks. Mechanistic studies continue to reveal the critical roles of ligand design, electronic effects, and substrate architecture in dictating selectivity and efficiency. Moving forward, the integration of computational modeling, expanded ligand libraries, and green oxidative systems will likely further enhance the scope and sustainability of these catalytic processes. Collectively, NHC–Au complexes are poised to remain at the forefront of enyne cycloisomerization, offering robust tools for both academic research and industrial innovation.

Conflicts of interest

There are no conflicts to declare.

Data availability

No primary research results, software, or code have been included, and no new data were generated or analyzed as part of this review.

Acknowledgements

We sincerely appreciate the Ministry of Higher Education and Scientific Research in Iraq for supporting this work.

References

- 1 K. Öfele, *J. Organomet. Chem.*, 1968, **12**, 42–43.
- 2 H. W. Wanzlick and H. J. Schönher, *Angew. Chem., Int. Ed.*, 1968, **7**, 141–142.
- 3 C. Romain, S. Bellemain-Lapoumaz and S. Dagorne, *Coord. Chem. Rev.*, 2020, **422**, 213411.
- 4 S. J. Hock, L.-A. Schaper, W. A. Herrmann and F. E. Kühn, *Chem. Soc. Rev.*, 2013, **42**, 5073–5089.
- 5 T. Scattolin and S. P. Nolan, *Trends in Chemistry*, 2020, **2**, 721–736.
- 6 L. A. Schaper, S. J. Hock, W. A. Herrmann and F. E. Kuehn, *Angew. Chem., Int. Ed.*, 2013, **52**, 270–289.
- 7 H. D. Velazquez and F. Verpoort, *Chem. Soc. Rev.*, 2012, **41**, 7032–7060.
- 8 D. Zhang and G. Zi, *Chem. Soc. Rev.*, 2015, **44**, 1898–1921.
- 9 P. Gao and M. Szostak, *Coord. Chem. Rev.*, 2023, **485**, 215110.
- 10 A. Jayaraj, A. V. Raveedran, A. T. Latha, D. Priyadarshini and P. C. A. Swamy, *Coord. Chem. Rev.*, 2023, **478**, 214922.
- 11 A. H. Mageed, *J. Organomet. Chem.*, 2019, **902**, 120965.
- 12 M. K. Pandey and J. Choudhury, *ACS Omega*, 2020, **5**, 30775–30786.
- 13 A. Doddi, M. Peters and M. Tamm, *Chem. Rev.*, 2019, **119**, 6994–7112.
- 14 V. Nesterov, D. Reiter, P. Bag, P. Frisch, R. Holzner, A. Porzelt and S. Inoue, *Chem. Rev.*, 2018, **118**, 9678–9842.
- 15 A. H. Mageed, B. W. Skelton, A. N. Sobolev and M. V. Baker, *Tetrahedron*, 2018, **74**, 2956–2966.
- 16 S. Diez-Gonzalez, N. Marion and S. P. Nolan, *Chem. Rev.*, 2009, **109**, 3612–3676.
- 17 T. Zhou, G. Utecht-Jarzyńska and M. Szostak, *Coord. Chem. Rev.*, 2024, **512**, 215867.
- 18 A. D'Amato, M. Sirignano, S. Russo, R. Troiano, A. Mariconda and P. Longo, *Catalysts*, 2023, **13**, 811.
- 19 A. H. Mageed and K. Al-Ameed, *RSC Adv.*, 2023, **13**, 17282–17296.
- 20 P. Bellotti, M. Koy, M. N. Hopkinson and F. Glorius, *Nat. Rev. Chem.*, 2021, **5**, 711–725.
- 21 H. M. Lee, C.-C. Lee and P.-Y. Cheng, *Curr. Org. Chem.*, 2007, **11**, 1491–1524.
- 22 M. Poyatos, J. A. Mata and E. Peris, *Chem. Rev.*, 2009, **109**, 3677–3707.
- 23 M. N. Hopkinson, C. Richter, M. Schedler and F. Glorius, *Nature*, 2014, **510**, 485–496.



24 F. He, K. P. Zois, D. Tzeli, A. A. Danopoulos and P. Braunstein, *Coord. Chem. Rev.*, 2024, **514**, 215757.

25 G. R. P. Vasu, K. R. M. Venkata, R. R. Kakarla, K. V. Ranganath and T. M. Aminabhavi, *Environ. Res.*, 2023, **225**, 115515.

26 Y.-F. Zhang, Y.-K. Yin, H. Zhang and Y.-F. Han, *Coord. Chem. Rev.*, 2024, **514**, 215941.

27 W. Zhao, V. Ferro and M. V. Baker, *Coord. Chem. Rev.*, 2017, **339**, 1–16.

28 A. H. Mageed and I. S. Hadi, *ChemistrySelect*, 2024, **9**, e202304737.

29 M. A. Hussein and A. Hassoon Mageed, *Asian J. Org. Chem.*, 2025, **14**, e202400528.

30 R. P. Herrera and M. C. Gimeno, *Chem. Rev.*, 2021, **121**, 8311–8363.

31 A. H. Mageed, B. W. Skelton and M. V. Baker, *Dalton Trans.*, 2017, 7844–7856.

32 S. Engel, E.-C. Fritz and B. J. Ravoo, *Chem. Soc. Rev.*, 2017, **46**, 2057–2075.

33 C. Eisen, J. M. Chin and M. R. Reithofer, *Chem.–Asian J.*, 2021, **16**, 3026–3037.

34 K. Al-Ameed and A. H. Mageed, *Polyhedron*, 2021, **205**, 115323.

35 A. H. Mageed, B. W. Skelton, A. N. Sobolev and M. V. Baker, *Eur. J. Inorg. Chem.*, 2018, **2018**, 109–120.

36 L. Rocchigiani and M. Bochmann, *Chem. Rev.*, 2020, **121**, 8364–8451.

37 R. Jouhannet, S. Dagorne, A. Blanc and P. de Frémont, *Chem.–Eur. J.*, 2021, **27**, 9218–9240.

38 D. Qian and J. Zhang, *Chem. Soc. Rev.*, 2015, **44**, 677–698.

39 M. Michalak and W. Kośnik, *Catalysts*, 2019, **9**, 890.

40 A. Collado, D. J. Nelson and S. P. Nolan, *Chem. Rev.*, 2021, **121**, 8559–8612.

41 A. Johnson and M. C. Gimeno, *Organometallics*, 2017, **36**, 1278–1286.

42 P. de Frémont, N. Marion and S. P. Nolan, *J. Organomet. Chem.*, 2009, **694**, 551–560.

43 M. V. Baker, P. J. Barnard, S. J. Berners-Price, S. K. Brayshaw, J. L. Hickey, B. W. Skelton and A. H. White, *J. Organomet. Chem.*, 2005, **690**, 5625–5635.

44 P. J. Barnard, M. V. Baker, S. J. Berners-Price and D. A. Day, *J. Inorg. Biochem.*, 2004, **98**, 1642–1647.

45 P. J. Barnard, M. V. Baker, S. J. Berners-Price, B. W. Skelton and A. H. White, *Dalton Trans.*, 2004, 1038–1047.

46 M. Monticelli, M. Baron, C. Tubaro, S. Bellemin-Laponnaz, C. Graiff, G. Bottaro, L. Armelao and L. Orian, *ACS Omega*, 2019, **4**, 4192–4205.

47 P. J. Barnard, L. E. Wedlock, M. V. Baker, S. J. Berners-Price, D. A. Joyce, B. W. Skelton and J. H. Steer, *Angew. Chem., Int. Ed.*, 2006, **45**, 5966–5970.

48 M. Baron, C. Tubaro, M. Basato, A. Biffis, M. M. Natile and C. Graiff, *Organometallics*, 2011, **30**, 4607–4615.

49 A. Neshat, P. Mastorilli and A. Mousavizadeh Mobarakeh, *Molecules*, 2021, **27**, 95.

50 E. Soriano and J. Marco-Contelles, *Computational Mechanisms of Au and Pt Catalyzed Reactions*, 2011, 1–29.

51 A. Arcadi, *Chem. Rev.*, 2008, **108**, 3266–3325.

52 D. J. Gorin, B. D. Sherry and F. D. Toste, *Chem. Rev.*, 2008, **108**, 3351–3378.

53 S. López, E. Herrero-Gómez, P. Pérez-Galán, C. Nieto-Oberhuber and A. M. Echavarren, *Angew. Chem.*, 2006, **118**, 6175–6178.

54 C. H. Amijs, C. Ferrer and A. M. Echavarren, *Chem. Commun.*, 2007, 698–700.

55 C. H. Amijs, V. Lopez-Carrillo, M. Raducan, P. Perez-Galan, C. Ferrer and A. M. Echavarren, *J. Org. Chem.*, 2008, **73**, 7721–7730.

56 J. P. Reeds, A. C. Whitwood, M. P. Healy and I. J. Fairlamb, *Organometallics*, 2013, **32**, 3108–3120.

57 J. P. Reeds, M. P. Healy and I. J. Fairlamb, *Catal. Sci. Technol.*, 2014, **4**, 3524–3533.

58 W. Wang, J. Yang, F. Wang and M. Shi, *Organometallics*, 2011, **30**, 3859–3869.

59 R. Harris and R. Widenhoefer, *Chem. Soc. Rev.*, 2016, **45**, 4533–4551.

60 K. Arumugam, B. Varghese, J. N. Brantley, S. S. Konda, V. M. Lynch and C. W. Bielawski, *Eur. J. Org. Chem.*, 2014, **2014**, 493–497.

61 A. S. F. León Rojas, S. H. Kyne and P. W. H. Chan, *Acc. Chem. Res.*, 2023, **56**, 1406–1420.

62 A. Mariconda, M. Sirignano, R. Troiano, S. Russo and P. Longo, *Catalysts*, 2022, **12**, 836.

63 A. G. Nair, R. T. McBurney, M. R. Gatus, S. C. Binding and B. A. Messerle, *Inorg. Chem.*, 2017, **56**, 12067–12075.

64 S. P. Nolan, *Acc. Chem. Res.*, 2011, **44**, 91–100.

65 R. Dorel and A. M. Echavarren, *Chem. Rev.*, 2015, **115**, 9028–9072.

66 B. M. Trost, M. Lautens, M. H. Hung and C. S. Carmichael, *J. Am. Chem. Soc.*, 1984, **106**, 7641–7643.

67 R. Grigg, P. Stevenson and T. Worakun, *Tetrahedron*, 1988, **44**, 4967–4972.

68 B. M. Trost and F. D. Toste, *J. Am. Chem. Soc.*, 2000, **122**, 714–715.

69 M. Méndez, M. P. Muñoz, C. Nevado, D. J. Cardenas and A. M. Echavarren, *J. Am. Chem. Soc.*, 2001, **123**, 10511–10520.

70 C. Nieto-Oberhuber, M. Muñoz-Herranz, E. Buñuel, C. Nevado, D. J. Cárdenas and A. M. Echavarren, *Angew. Chem., Int. Ed.*, 2004, **43**, 2402–2406.

71 S. M. Kim, J. H. Park, S. Y. Choi and Y. K. Chung, *Angew. Chem.*, 2007, **119**, 6284–6287.

72 M. Gaydou, R. E. Miller, N. Delpont, J. Cecon and A. M. Echavarren, *Angew. Chem.*, 2013, **52**, 6396–6399.

73 P. Calleja, Ó. Pablo, B. Ranieri, M. Gaydou, A. Pitaval, M. Moreno, M. Raducan and A. M. Echavarren, *Chem.–Eur. J.*, 2016, **22**, 13613–13618.

74 Y. Matsumoto, K. B. Selim, H. Nakanishi, K.-i. Yamada, Y. Yamamoto and K. Tomioka, *Tetrahedron Lett.*, 2010, **51**, 404–406.

75 B. W. Gung, M. R. Holmes, C. A. Jones, R. Ma and C. L. Barnes, *Tetrahedron Lett.*, 2016, **57**, 3912–3915.

76 K. Usui, T. Yoshida and M. Nakada, *Tetrahedron: Asymmetry*, 2016, **27**, 107–113.



77 N. Okitsu, T. Yoshida, K. Usui and M. Nakada, *Heterocycles*, 2016, **92**, 720–732.

78 J.-Q. Zhang, Y. Liu, X.-W. Wang and L. Zhang, *Organometallics*, 2019, **38**, 3931–3938.

79 H. F. Jónsson, A. Orthaber and A. Fiksdahl, *Dalton Trans.*, 2021, **50**, 5128–5138.

80 A. Simonneau, Y. Harrak, L. Jeanne-Julien, G. Lemiere, V. Mouriès-Mansuy, J. P. Goddard, M. Malacria and L. Fensterbank, *ChemCatChem*, 2013, **5**, 1096–1099.

81 W. Zang, L. Wang, Y. Wei, M. Shi and Y. Guo, *Adv. Synth. Catal.*, 2019, **361**, 2321–2328.

82 R. Laher, C. Marin and V. Michelet, *Org. Lett.*, 2020, **22**, 4058–4062.

83 R. Laher, E. Gentilini, C. Marin and V. Michelet, *Synthesis*, 2021, **53**, 4020–4029.

84 B. S. Kale, H. F. Lee and R. S. Liu, *Adv. Synth. Catal.*, 2017, **359**, 402–409.

85 P. Zhang, C. Tugny, J. M. Suárez, M. Guitet, E. Derat, N. Vanthuyne, Y. Zhang, O. Bistri, V. Mouriès-Mansuy and M. Ménand, *Chem*, 2017, **3**, 174–191.

86 P. Zhang, C. Tugny, J. M. Suárez, M. Guitet, E. Derat, N. Vanthuyne, Y. Zhang, O. Bistri, V. Mouriès-Mansuy, M. Ménand Tugny, N. del Rio, M. Koohgard, N. Vanthuyne, D. Lesage, K. Bijouard, P. Zhang, J. Meijide Suárez, S. Roland, O. Bistri-Aslanoff, M. Sollogoub, L. Fensterbank and V. Mouriès-Mansuy, *ACS Catal.*, 2020, **10**, 5964–5972.

87 G. Xu, O. Bistri-Aslanoff, V. Mouriès-Mansuy, L. Fensterbank, Y. Zhang, S. Roland and M. Sollogoub, *Eur. J. Org. Chem.*, 2025, e202401378.

88 L. Pallova, L. Abella, M. Jean, N. Vanthuyne, C. Barthes, L. Vendier, J. Autschbach, J. Crassous, S. Bastin and V. César, *Chem. -Eur. J.*, 2022, **28**, e202200166.

89 G. Wang, Y. Wang, Z. Li, H. Li, M. Yu, M. Pang and X. Zhao, *Org. Lett.*, 2022, **24**, 9425–9430.

90 G. Wang, H. Li, Y. Wang, Z. Li, G. Liu and X. Zhao, *Org. Chem. Front.*, 2023, **10**, 5705–5709.

91 R. Heinrich, G. Marie-Rose, C. Gourlaouen, P. Pale, E. Brenner and A. Blanc, *Chem. -Eur. J.*, 2025, e202404446.

92 A. Pradal, Q. Chen, P. F. dit Bel, P. Y. Toullec and V. Michelet, *Synlett*, 2012, **2012**, 74–79.

93 V. López-Carrillo, N. Huguet, A. Mosquera and A. M. Echavarren, *Chem. -Eur. J.*, 2011, **17**, 10972–10978.

94 G.-Q. Chen, W. Fang, Y. Wei, X.-Y. Tang and M. Shi, *Chem. Sci.*, 2016, **7**, 4318–4328.

95 J. P. Reeds, A. C. Whitwood, M. P. Healy and I. J. Fairlamb, *Chem. Commun.*, 2010, **46**, 2046–2048.

96 P. T. Bohan and F. D. Toste, *J. Am. Chem. Soc.*, 2017, **139**, 11016–11019.

97 J. Rodriguez and D. Bourissou, *Angew. Chem.*, 2017, **57**, 386–388.

98 C.-Y. Wu, T. Horibe, C. B. Jacobsen and F. D. Toste, *Nature*, 2015, **517**, 449–454.

99 J. S. Lee, E. A. Kapustin, X. Pei, S. Llopis, O. M. Yaghi and F. D. Toste, *Chem*, 2020, **6**, 142–152.

100 M. Koohgard, L. Enders, N. Del Rio, H. Li, F. Moccia, O. Khaled, O. Bistri, J. Helaja, M. Sollogoub and V. Mouriès-Mansuy, *Org. Lett.*, 2024, **26**, 5817–5821.

101 A. Cataffo, M. Peña-López, R. Pedrazzani and A. M. Echavarren, *Angew. Chem., Int. Ed.*, 2023, **62**, e202312874.

102 K. Wittstein, K. Kumar and H. Waldmann, *Angew. Chem.*, 2011, **39**, 9242–9246.

103 W. Zang, Y. Wei and M. Shi, *Chem. Commun.*, 2019, **55**, 8126–8129.

104 X. Chen, A. T. Holm and P. W. H. Chan, *Aust. J. Chem.*, 2020, **73**, 1165–1175.

105 X. Chen, C. A. Baratay, M. E. Mark, X. Xu and P. W. Hong Chan, *Org. Lett.*, 2020, **22**, 2849–2853.

106 B. Ranieri, C. Obradors, M. Mato and A. M. Echavarren, *Org. Lett.*, 2016, **18**, 1614–1617.

107 Y.-J. Wang, X.-X. Li and Z. Chen, *J. Org. Chem.*, 2020, **85**, 7694–7703.

108 C. A. Witham, P. Mauleón, N. D. Shapiro, B. D. Sherry and F. D. Toste, *J. Am. Chem. Soc.*, 2007, **129**, 5838–5839.

109 L. Ricard and F. Gagasz, *Organometallics*, 2007, **26**, 4704–4707.

110 D. Qian and J. Zhang, *Chem. Commun.*, 2011, **47**, 11152–11154.

111 D. Vasu, H.-H. Hung, S. Bhunia, S. A. Gawade, A. Das and R.-S. Liu, *Angew. Chem., Int. Ed.*, 2011, **50**, 6911–6914.

112 A. Homs, M. E. Muratore and A. M. Echavarren, *Org. Lett.*, 2015, **17**, 461–463.

113 K.-B. Wang, R.-Q. Ran, S.-D. Xiu and C.-Y. Li, *Org. Lett.*, 2013, **15**, 2374–2377.

114 H. H. Hung, Y. C. Liao and R. S. Liu, *Adv. Synth. Catal.*, 2013, **355**, 1545–1552.

115 S. Ferrer and A. M. Echavarren, *Angew. Chem.*, 2016, **128**, 11344–11348.

116 S. Ferrer and A. M. Echavarren, *Synthesis*, 2019, **51**, 1037–1048.

117 W. Fang, X.-Y. Tang and M. Shi, *RSC Adv.*, 2016, **6**, 40474–40479.

118 B. Jiang, Y. Wei and M. Shi, *Org. Chem. Front.*, 2018, **5**, 2091–2097.

119 Z.-Z. Zhou, Y.-J. Wang, Q. Zou and Z. Chen, *Tetrahedron Lett.*, 2024, **136**, 154918.

